

THE MEASUREMENT OF THE FAST NEUTRON FLUX AT THE FAST
BEAM PORT OF THE KSU TRIGA MARK II REACTOR

by

445

Kenneth Edward Habiger

B. S., Kansas State University, 1964

A MASTER'S THESIS

submitted in partial fulfillment of the
requirements for the degree

MASTER OF SCIENCE

Department of Nuclear Engineering

KANSAS STATE UNIVERSITY
Manhattan, Kansas

1966

Approved by:


Major Professor

LD
2668
T4
1966
H 116
C. 2
Document

TABLE OF CONTENTS

INTRODUCTION.....	1
THEORY.....	4
The Neutron Energy Spectrum from Fission of Uranium-235.....	4
Fast Neutron Scintillation Spectrometry.....	8
Neutron Spectrum Unfolding.....	10
Error Analysis.....	14
EXPERIMENTAL FACILITIES.....	17
Equipment for Pulse Height Analysis.....	20
Other Facilities.....	23
EXPERIMENTAL PROCEDURE.....	25
Adjusting the Linear Amplifiers and the Multichannel Analyzer...	30
Adjusting the Variable Delay.....	33
Procedure for Taking Data.....	33
DISCUSSION AND RESULTS.....	35
Neutron Spectrum Unfolding Tests.....	35
Po-Be Neutron Spectra.....	39
Reactor Neutron Spectra.....	46
CONCLUSIONS.....	57
SUGGESTIONS FOR FURTHER STUDY.....	59
ACKNOWLEDGMENT.....	61
LITERATURE CITED.....	62

APPENDICES.....	64
APPENDIX A: Absolute Differential Efficiency as a Function of Light Output (in "Cobalt" Units) for Plane Parallel Monoenergetic Neutrons Perpendicular to Axes of 2" x 2" Diameter Cylinder of NE-213 Scintillator.....	65
APPENDIX B: Description and Explanation of the IBM-1410 Computer Program Used for Calculation of the Response Functions.....	74
APPENDIX C: Explanation of the Input Routines for the IBM-1410 Unfolding Code Being Developed in the KSU Department of Nuclear Engineering.....	80
APPENDIX D: Letter Received from Oak Ridge National Laboratory Regarding KSU Data Analysis.....	82
APPENDIX E: Modifications in the B. J. Electronics A8 Amplifier.....	86

LIST OF TABLES

I. Properties of Liquid NE-213.....	17
II. Optimum Photomultiplier Voltage Determination.....	27
III. Modified A8 and Forte Resistance Potentiometer Settings.....	29
IV. Low Gain Test Spectrum Containing Two Neutron Energies.....	36
V. Low Gain Test Spectrum Containing Eleven Neutron Energies.....	37
VI. High Gain Test Spectrum Containing Twelve Neutron Energies.....	38
B-I. Input and Output Parameters Required for Execution of CONVERT..	74
C-I. Input Routines for KSU Department of Nuclear Engineering Unfolding Code.....	81

LIST OF FIGURES

1. Experimental and calculated uranium-235 fission spectrum.....	6
2. Neutron energy spectrum at the core of the KSU TRIGA Mark II reactor.....	7
3. Absolute differential efficiency for a 2" x 2" diam NE-213 scintillator for neutron energies shown.....	12
4. Absolute differential efficiency for a 2" x 2" diam NE-213 scintillator for neutron energies shown.....	13
5. Forte pulse-shape discrimination circuit.....	19
6. Detector assembly and Forte pulse shape discrimination circuit...	21
7. Pulse height analysis equipment.....	22
8. Detector assembly in front of collimated beam port.....	24
9. Pulse heights from Po-Be and Co ⁶⁰ gamma-rays vs. photomultiplier tube voltage.....	26
10. Test of amplifier linearity.....	31
11. Low gain Po-Be complex neutron spectrum.....	40
12. Low gain Po-Be complex and smoothed spectra.....	41
13. High gain Po-Be complex neutron spectrum.....	42
14. Comparison of KSU Po-Be spectrum to ORNL Po-Be spectrum.....	44
15. Unfolded Po-Be spectrum with theoretical curve by Whitmore and Baker (23).....	45
16. One watt low gain reactor complex spectrum.....	48
17. One watt low gain reactor complex and smoothed spectra.....	49
18. One watt high gain reactor complex spectrum.....	50

19. Five watt low gain reactor complex spectrum.....	51
20. Five watt low gain reactor complex and smoothed spectra.....	52
21. Five watt high gain reactor complex spectrum.....	53
22. Five watt high gain reactor complex spectrum at 2400 photomultiplier volts.....	54
23. Unfolded 1 watt reactor neutron spectrum with theoretical curve of Joanou and Dudek (12).....	55
24. Unfolded 5 watt reactor neutron spectrum with theoretical curve of Joanou and Dudek (12).....	56
25. Logic diagram for program used to calculate the response functions.....	76

NOMENCLATURE

A	Response matrix of the spectrometer system to monoenergetic neutrons
A^T	Transpose of A
E	Neutron energy
C	$A^T \omega A$
I	Unit matrix

Greek Symbols

β	Neutron flux
ρ	Number of counts in a channel of a multichannel analyzer
σ^2	Mean square deviation of ρ
ω	Weighting matrix

INTRODUCTION

The ideal neutron spectrometer would have high efficiencies over all neutron energies, good resolution, be insensitive to gamma and beta radiation, yield distinct lines for monoenergetic neutrons, require simple electronics, and be inexpensive. No spectrometer yet developed has all these desired qualities.

Several neutron spectrometers developed in the past have been successful in limited applications. Typical of these are the nuclear emulsion (2) and the hydrogen cloud chamber (4). Both displayed good resolution and fairly good background discrimination, but were plagued with poor efficiency due to the tedious task of measuring neutron track lengths. Adelson et al. (1) described a hydrogen bubble chamber that was useful as a neutron spectrometer in the 5 to 30 Mev range, but with no inherent gamma discrimination capabilities.

The use of Lithium-Iodide scintillation crystals in the thermal neutron range has been suggested by Price (18) who notes the high detection efficiency of LiI in this energy range. Moreover, Murray (15) reports favorable responses of LiI to neutrons in the 1 to 14 Mev range. The main disadvantage of LiI as a neutron spectrometer is its high efficiency for gamma radiation.

The He-3 proportional counter is described by Batchelor et al. (3) as a suitable neutron spectrometer for energies from thermal to 1 Mev. Above 1 Mev elastic collisions between neutrons and He-3 nuclei become important and the total energy given off by the interaction is no longer linearly related to the energy of the incident neutron. However, the He-3

proportional counter is not sensitive to gamma-ray radiation.

Time of flight measurements have been applied in neutron spectrometry (16) with considerable success in the low to moderately high neutron energies. However, at energies above a few Mev, time of flight displays poor resolution due to inadequacy of flight time measuring equipment. Time of flight spectrometers also suffer from lack of a gamma discrimination scheme.

M. J. Poole (17) was one of the first to describe a technique for deriving neutron spectra from proton recoils in the inelastic scattering of neutrons. E. A. Eliot et al. (9) also suggested the use of proton recoils in the stilbene neutron spectrometer. Both of these methods relied on subtraction of background to eliminate gamma radiation and were, thus, generally inaccurate. Johnson and Trail (13) described a proton recoil spectrometer system that was good in the 2 to 20 Mev range, but was also sensitive to gamma radiation. J. E. Draper (7) suggested a proton recoil spectrometer capable of discriminating against gammas by a coincidence technique utilizing two crystals. However, the coincidence requirement resulted in very low efficiencies, and the resulting neutron pulse height distribution had to be analyzed, or unfolded, to obtain the true neutron spectrum.

It is evident that all the neutron spectrometers discussed above are characterized by one disadvantage or another. The main disadvantages are sensitivity to gamma radiation, poor efficiency, limited energy range, and in the case of proton recoil spectrometers, difficult pulse height analysis.

Recently, techniques have been developed that can circumvent the gamma radiation problem. Broek and Anderson (5) have reported measuring neutron spectra by the proton recoil method in the energy range 1 to 10 Mev using stilbene crystals capable of pulse shape discrimination to eliminate gammas. Stilbene has good resolution, but has the disadvantage of being non-isotropic, so that its use depends on the orientation of its axis with respect to the incident neutrons.

More recently, Burrus and Verbinski (6) have investigated the use of the organic scintillator NE-213, which also is capable of pulse shape discrimination. It has somewhat poorer resolution than stilbene, but does not display a non-isotropic character and has relatively high efficiency for neutrons in the 0.5 to 14 Mev range. Burrus and Verbinski (6) also describe a method of analyzing, or unfolding, the resulting pulse height to obtain the unscrambled spectrum. This unfolding technique is based on the measurement of the response of NE-213 to at least two mono-energetic neutrons (22).

An NE-213 spectrometer system similar to that of Burrus and Verbinski has been assembled at Kansas State University for fast neutron spectrum analysis. The purpose of the work described here is to develop operating procedures for this system, determine the system operating characteristics, and apply the system to the measurement of the fast neutron energy spectrum of Po-Be and of reactor neutrons at the fast beam port of the KSU TRIGA Mark II reactor.

THEORY

The Neutron Energy Spectrum from Fission of Uranium-235

Many nuclear reactions involving the emission of a light particle or gamma-ray had been carried out prior to 1939. In that year, however, nuclear fission was discovered while attempting to produce transuranium elements by bombarding uranium with low energy or slow neutrons (14).

We now know that the slow neutron fission process in uranium can be principally attributed to the isotope uranium-235, which is present to the extent of 0.712 per cent in natural uranium (10). Uranium-235 fission generally results in the production of two fission fragments of about equal weight and, in addition, an average of 2.5 neutrons per fission.

The neutrons given off in the fission process can be classified in the following manner:

1. prompt fission neutrons emitted within a few microseconds of the fission event
2. delayed fission neutrons emitted from β^- active fission products.

The delayed neutrons represent a small fraction of the total neutrons given off and are generally grouped in energies below 0.5 Mev. This is below the energy range considered in the present work and for this reason only the prompt fission neutrons need be considered.

The prompt neutrons given off in uranium-235 fission have a spectrum of energies ranging from about 0.25 to 18.0 Mev. The spectrum can be approximated analytically by the expression (19)

$$N(E) = \sqrt{2/\pi e} \sinh \sqrt{2E} e^{-E}$$

where $N(E)$ = fraction of neutrons per unit energy range emitted per fission

E = neutron energy in Mev.

The uranium-235 neutron fission spectrum has also been measured experimentally. The measured spectrum presented by Goldstein (11) is reproduced in Fig. 1 along with a calculated curve using the above expression.

The neutron spectrum one would find in the core of a reactor differs from the true fission spectrum due to interaction of the neutrons with absorbing and moderating materials present in the core. The neutron spectrum in any core then depends on the nuclear properties of the material in that core.

The principal materials in the TRIGA Mark II core are uranium-235, uranium-238, aluminum, hydrogen, oxygen, and zirconium. Joanou and Dudek (12) have calculated the neutron spectrum for the TRIGA core based on these materials using a P_1 approximation of the time-independent Boltzman equation. The results of their calculations are plotted in Fig. 2.

Although the neutron spectrum for the TRIGA plotted in Fig. 2 has been calculated specifically for the core, it should be a very good approximation to the spectrum at the fast beam port. There is a void in the reflector between the core and the fast beam port. Thus, the only materials that can attenuate the neutrons that eventually enter the fast beam port are the thin reactor tank and the air in the port. Some scattering will take place in the port, but if a collimator is used in making spectrum determinations, the resulting spectrum should be that of an

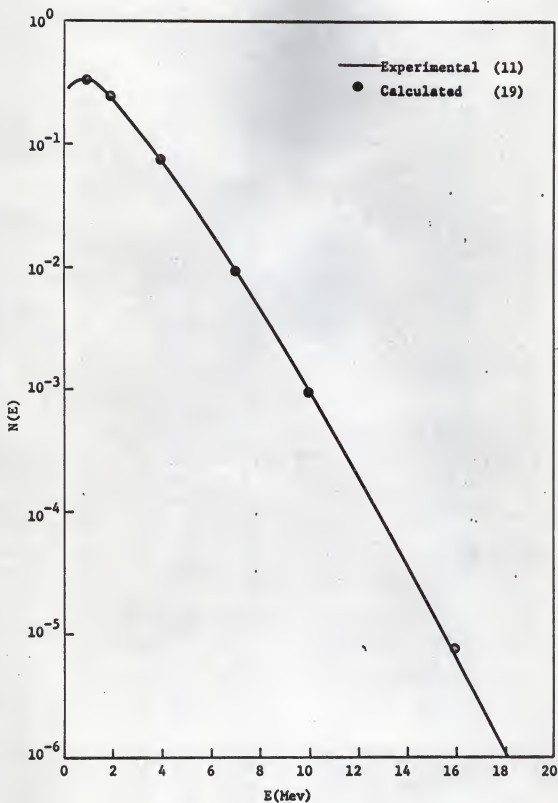


Figure 1. Experimental and calculated uranium-235 fission spectrum (11, 19)

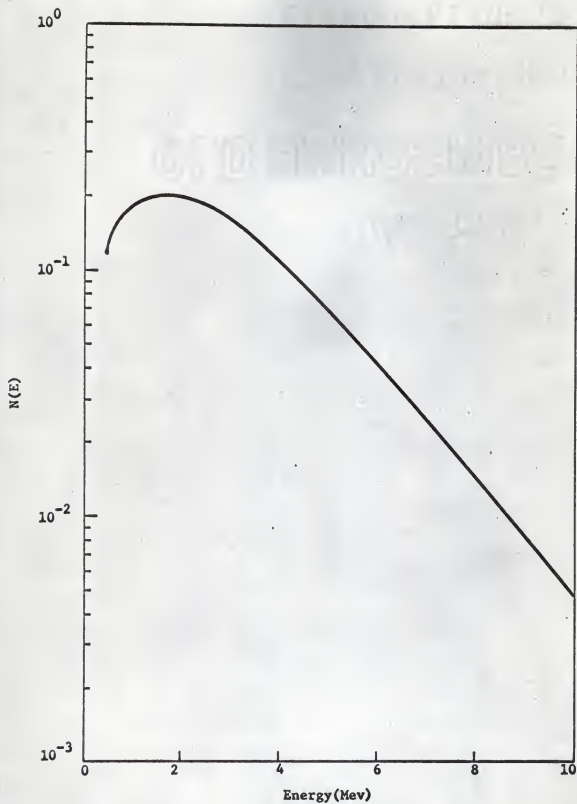


Figure 2. Neutron energy spectrum at the core of the KSU TRIGA Mark II reactor (12)

essentially, uncollided flux. The spectrum determined in this work is compared to the spectrum calculated by Joanou and Dudek (12) (see Fig. 2).

Fast Neutron Scintillation Spectrometry

Neutrons are uncharged particles and do not lose energy by direct ionization of the matter through which they pass. However, neutron detection devices, like most radiation monitors, must be activated by ionized matter; in the neutron case the ions are produced by a charged particle resulting from a neutron-nucleus interaction. Neutron interactions that result in ionizing charged particles can be classified in the following categories (14):

1. the absorption of a neutron by a nucleus followed by the prompt emission of a fast charged particle
2. the absorption of a neutron followed by fission of the absorbing nucleus
3. the scattering of a neutron by a light nucleus, such as a proton, with the recoiling light nucleus producing ionization.

The first two interactions are most common to slow neutrons and, thus, will not be considered here. The last interaction, referred to as a "proton recoil" interaction, is most commonly utilized in the detection of fast neutrons and is the basis for fast neutron scintillation spectrometry. Detection is based on noting the ionization caused by recoiling protons produced in the elastic scattering of neutrons by hydrogenous materials.

To understand neutron scintillation spectrometry, it is convenient

to review the scintillation process. The operation of a fast neutron scintillation detector can be divided into six consecutive events (18); these are:

1. scattering of a neutron by a proton in the scintillator, with the proton producing ionization within the scintillator
2. conversion of energy lost in the scintillator to light energy through the luminescence process
3. movement of the light photons to the photocathode of the photomultiplier tube
4. absorption of light photons at the photocathode with subsequent emission of photoelectrons
5. multiplication of electrons within the photomultiplier tube
6. analysis of the resulting current pulse from the photomultiplier tube with appropriate electronic equipment.

The proton recoils produced in the first event lose their energy by several different processes. The processes are complex and not well understood, but are generally believed to include exciton migration, sensitized fluorescence, and photon emission and reabsorption (18). The processes can be thought of as the transfer of energy from proton recoils to scintillator molecules, the latter being transferred from the electronic ground state to an excited state. This excitation energy is subsequently radiated as fluorescent radiation in the second event.

As light photons strike the photocathode, photoelectrons are given off in accordance with the principles of photoelectron emission. These

photoelectrons are accelerated by a voltage gradient to a dynode where secondary electrons are given off. Secondary emission occurs when electrons bombard an electron emitting surface such as cesium-antimonide with an energy of approximately 100 volts. The overall amplification of a photomultiplier is achieved by placing several dynodes in series where the secondary electrons from one dynode become the incident electrons for the next.

The final step in the photomultiplier process occurs at the anode where the electrons are collected. The resulting current pulse is led to a pre-amplifier, then to a linear amplifier, and finally to a multichannel analyzer. The spectrum obtained from the multichannel analyzer however, will not be the true energy spectrum; photomultiplier efficiency, instrument distortion, and indirect neutron-proton collisions with less than total energy conversion will smear the true spectrum. The true spectrum must be "unfolded" from the smeared spectrum by spectrum analysis. A method of unfolding is presented in the next section.

Neutron Spectrum Unfolding

As described above, the spectrum obtained from the scintillation detector and multichannel analyzer will not be the true spectrum; limitations in the system and counting statistics will smear the true spectrum. The resulting complex spectrum must be analyzed or "unfolded" to obtain the actual spectrum.

The unfolding method presented here was formulated by Trombka (21) for the analysis of gamma-ray pulse height; this method will be applied

to neutron spectrum unfolding since the principles are the same in both cases.

The number of counts ρ_i in any channel i of the multichannel analyzer-scintillation detector system exposed to a neutron flux can be given by

$$\rho_i = \sum_E A_i(E) \beta(E) \quad (1)$$

where $A_i(E)$ = probability that a unit intensity source of energy E will result in a count in channel i

$\beta(E)$ = neutron flux.

The $A_i(E)$'s are generally referred to as "response functions" and are the response of the detection system to neutrons of energy E . Response of NE-213 liquid scintillator has been measured and/or calculated for 12 monoenergetic neutron energies by Oak Ridge National Laboratory (22). These responses are plotted in Figures 3 and 4.

Equation 1 can be re-written in matrix form as

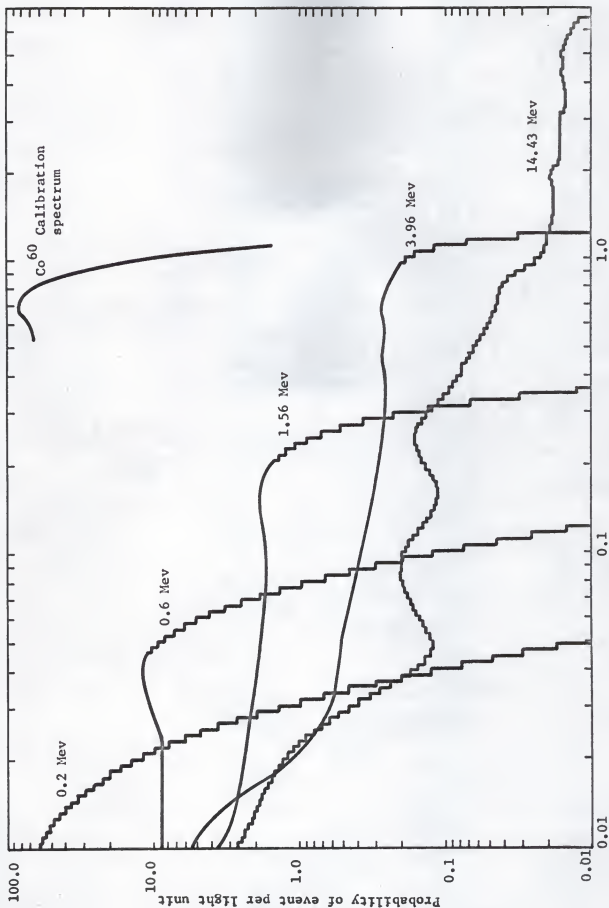
$$\rho = A\beta \quad (2)$$

or

$$A\beta = \rho. \quad (3)$$

Because of statistical errors in the measurement of ρ , it is not possible to invert A and proceed directly to the solution for β . Instead, a least squares solution is used to minimize the effects of these errors.

The solution for β in the least squares sense can be obtained by multiplying both sides of Eq. (3) by the transpose of A . The solution is



Pulse height (light units)

Figure 3. Absolute differential efficiency for a 2" x 2" diam NE-213 scintillator for neutron energies shown

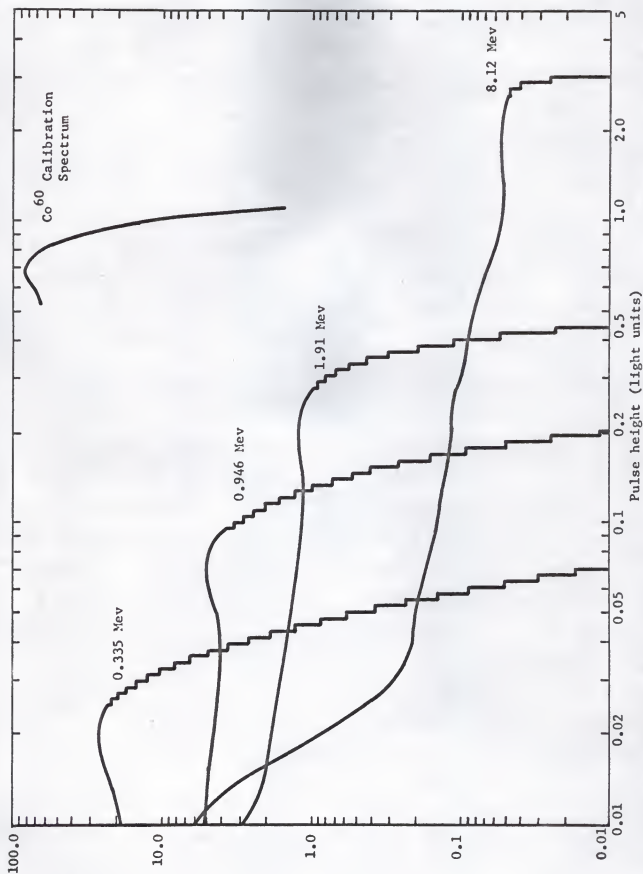


Figure 4. Absolute differential efficiency for a 2" x 2" diam NE-213 scintillator for neutron energies shown

$$\beta = (A^T \omega A)^{-1} A^T \omega \rho \quad (4)$$

where a weighting matrix ω has been included. The application of least squares principles requires that the variance of each observation be the same. Since the variance in each element of ρ will be different, an attempt must be made to place equal variance on each observation. The diagonal weighting matrix ω attempts to do this by letting $\omega_{ii} = 1/\sigma_i^2$ where σ_i^2 is the mean square deviation of ρ_i . The calculation described in Eq. (4) has been programmed by Eckhoff and Hill (8) for the IBM 1410 computer; this computer has more than enough capacity to handle the 12 monoenergetic neutron pulse height spectra and 200 channels used in this experiment.

Error Analysis

Once the β 's in Eq. (4) have been determined, it is possible to calculate the mean square deviation in β . This calculation is rather simple in the case where it is assumed that the A_{ij} 's (monoenergetic pulse height spectra) are known without error.

Equation 4 can be written as

$$\beta_n = \sum_{ik} C_{nk}^{-1} A_{ik} \omega_i \rho_i \quad (5)$$

where

$$C = A^T \omega A$$

or

$$C_{jk} = \sum_i \omega_i A_{ij} A_{ik} \quad (6)$$

The inverse of C is given by C^{-1} ; then $CC^{-1} = I$ where I is the identity matrix with elements I_{jn} and

$$I_{jn} = \sum_k C_{jk} C_{kn}^{-1}. \quad (7)$$

The elements of " I " have the values

$$\begin{aligned} I_{jn} &= 1 & \text{if } j &= n \\ I_{jn} &= 0 & \text{if } j \neq n. \end{aligned} \quad (8)$$

The mean square deviation $\sigma^2(\beta_n)$ corresponding to the deviation in ρ_1 can be written as

$$\sigma^2(\beta_n) = \sum_{ijk} \sum_l \sum_m C_{jn}^{-1} C_{kn}^{-1} A_{lj} A_{ik} \omega_l^2 \sigma^2(\rho_1). \quad (9)$$

When $\omega_1 = 1/\sigma_1^2(\rho_1)$, Eq. (8) becomes

$$\sigma^2(\beta_n) = \sum_{ijk} \sum_l \sum_m C_{jn}^{-1} C_{kn}^{-1} A_{lj} A_{ik} \omega_l \quad (10)$$

or

$$\sigma^2(\beta_n) = \sum_{jk} C_{jn}^{-1} C_{kn}^{-1} A_{1j} A_{1k} \omega_1. \quad (11)$$

Using Eq. (6):

$$\sigma^2(\beta_n) = \sum_{jk} C_{jn}^{-1} C_{kn}^{-1} C_{jk} \quad (12)$$

or

$$\sigma^2(\beta_n) = \sum_j C_{jn}^{-1} \sum_k C_{jk} C_{kn}^{-1}. \quad (13)$$

Then from Eqs. (7) and (8)

$$\sigma^2(\beta_n) = C_{nn}^{-1}. \quad (14)$$

Equation (14) states that the mean square deviations in β are contained on the diagonal of the C^{-1} matrix. If the response matrix is known without error and the counting time is the same for all ρ_i 's, the mean square deviation in ρ_i is given by

$$\sigma^2(\rho_i) = \rho_i. \quad (15)$$

EXPERIMENTAL FACILITIES

The liquid scintillator used in this work is known as NE-213 (20); the liquid scintillation detector assembly is a 2 in. diameter by 2 in. high cylindrical glass cell containing 103 cc. of NE-213. Purchased from the Harshaw Chemical Co., the scintillation liquid was deoxygenated and encapsulated under nitrogen at the factory. One end of the glass encapsulation cell is ground flat and polished for optical contact. The upper portion of the cell is covered with a thin coating of diffuse white reflector paint.

NE-213 scintillation liquid, prepared from purified xylene, naphthalene, activators and POPOP spectrum shifter, is designed for internal counting investigations and formulated to minimize the quenching action of added materials. This scintillator has pulse shape discrimination capabilities similar to stilbene and is particularly useful for neutron counting in the presence of gamma radiation. Other properties of NE-213 are shown in Table I (20).

Table I

Properties of Liquid NE-213

Density	Refractive Index	Boiling Pt.	Light Output (% Anthracene)	Decay Constant Main Component
0.88	1.508	141°C	78	2.4×10^{-9} sec

Response of liquid NE-213 to monoenergetic neutrons has been reported

by Verbinski et al. (22) for two cylindrical cell sizes; this response is referenced to the light output from a Co^{60} source. "One Cobalt" is the point at which the extrapolated Compton edge for the combined 1.17 and the 1.33 Mev Co^{60} gamma spectrum crosses the abscissa. Response of NE-213 is shown in Fig. 3 and Fig. 4 for a 2 in. diameter by 2 in. high cell.

The photomultiplier and pulse shape discrimination circuits used are duplicates of systems now in use at Oak Ridge National Laboratory. An RCA type 6810-A photomultiplier tube is used; a schematic of the pulse shape discrimination circuit, or "Forte circuit", is shown in Fig. 5 (reproduced from a publication by ORNL (6)).

A linear signal containing components from both neutrons and gammas is taken from the 10th dynode of the phototube for pulse height analysis. The anode signal is clipped using a delay cable and the negative portion is fed to a summing network where it is added to the positive signal from the 14th phototube dynode. This positive signal cannot effectively overcome the negative signal in the case of a gamma ray, and the gamma ray pulse is canceled out. The slow positive pulse resulting from a proton recoil, however, is too large to be canceled by the clipped negative pulse and the result is a net positive pulse. This positive signal, or gating pulse, admits neutron counts to the multichannel analyzer when it appears in coincidence with the linear signal; when the gating pulse is not present the linear pulse is rejected and gamma ray counts are eliminated.

The scintillator bottle is optically coupled to the phototube with



Dow Corning 10^6 centistokes silicone compound. A small portion of the grease is placed on the end of the phototube; the scintillator bottle is then placed directly on the grease and turned until all streaks and air bubbles are eliminated. The optically coupled phototube and scintillator bottle are then wrapped with black plastic electricians tape to insure a light-tight system. (See Fig. 6 for a picture of the detector assembly and Forte circuit.)

Equipment for Pulse Height Analysis

As noted above, a linear signal from the 10th phototube dynode is used for pulse height analysis. This signal is led to a B. J. Electronics Model DA8 linear amplifier. During neutron spectrum analysis the amplifier is operated at several different gains to obtain optimum resolution for both high and low energy neutrons. Amplified output from the linear amplifier is delayed 2 microseconds with a delay device; output from the delay device is led to the high level input of a TMC 256 multichannel analyzer with Model 210 pulse height logic unit (see Fig. 7).

The pulse shape discriminator (PSD) output is led to a modified B. J. Electronics Model DA8 linear amplifier. This amplifier is modified to provide a 10 volt positive pulse with a rise and fall time of 0.3 microseconds (see Appendix E). The positive pulse is used to gate the multichannel analyzer. Linear and gating pulses must be in coincidence to eliminate gamma-ray counts.



Figure 6. Detector assembly and Forte pulse shape discrimination circuit



Figure 7. Pulse height analysis equipment

Power required for the PSD and photomultiplier circuits is obtained from a John Fluke Model 400BDA power supply; a regulated voltage is supplied to the amplifiers by a Beckman Voltage Regulator, Model 760R.

Other Facilities

The very high voltages applied to the phototube require that the tube be shielded to prevent static noise pulses from swamping the neutron pulses. Two concentric metal cylinders, 10 inches long, purchased from the Magnetic Shield Division of the Perfection Mica Company, shield the phototube; these cylinders reduce the noise to acceptable levels. The inner cylinder is constructed of 0.031 in. CO-NETIC AA material, and is 2 1/2" I.D.; the outer cylinder is constructed of 0.031 in. NETIC S3-6 material and is 2 13/16" I.D. A 9/16" thick sheet of polyethylene separates the two cylinders.

During neutron spectrum measurements the photomultiplier and Forte circuit assemblies are mounted on a stand (see Fig. 8); horizontal and vertical adjustments of this stand are made to insure that the detector is centered in the neutron beam. The neutron beam is collimated to a 1 1/4" x 1 1/4" beam as it emerges from the beam port; the beam spreads to a 3" x 3" size 8' from the exit point. The detector assembly is placed at the 8 foot point to insure uniform irradiation of the 2" x 2" detector.

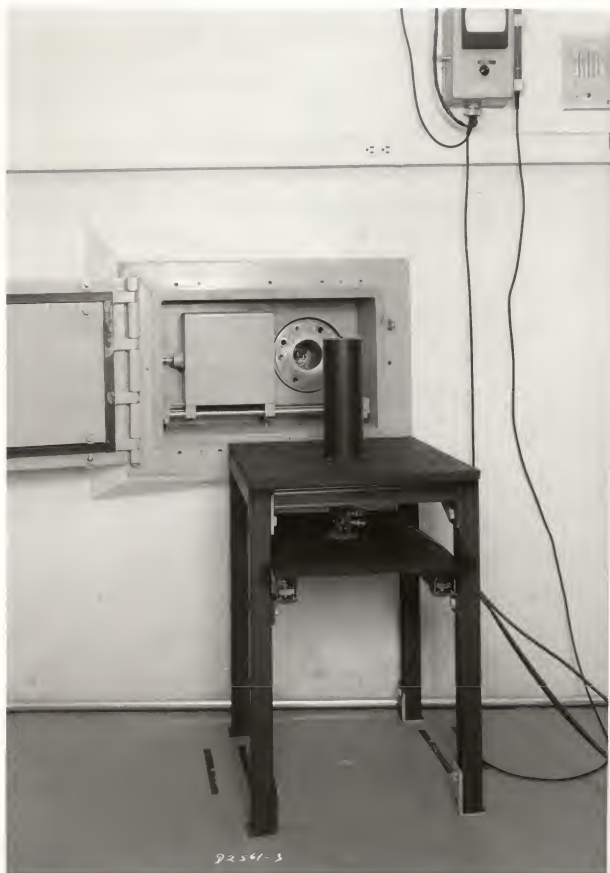


Figure 8. Detector assembly in front of collimated beam port

EXPERIMENTAL PROCEDURE

There are three possible adjustments that can be made in the Fortephotomultiplier circuits; these variables must be properly set if optimum counting is to be obtained. The first adjustment to be considered is the photomultiplier tube voltage. If the applied voltage is too high, the tube will go into a state of saturation when a high energy neutron enters the detector. This saturation will distort the high energy end of the neutron spectrum, i.e. the highest energy neutrons will be counted as neutrons of a lower energy. If the applied voltage is too low, the low energy neutron pulses will not be detected and the low energy end of the spectrum will be distorted.

The optimum phototube voltage is determined by plotting the ratio of pulse heights of 4.43 Mev Po-Be gammas to the gammas of a Co^{60} source against photomultiplier tube voltage. Phototube voltage is increased until the 4.43 Mev gamma shows saturation and the ratio of pulse heights from Po-Be to Co^{60} falls off. The pulse height of the 4.43 Mev gamma is noted at this voltage. Tube voltage is then decreased until the 4.43 Mev pulse height is approximately half of its saturation value. This is a safe operating voltage for 14 Mev neutrons, since they have pulse heights approximately equal to that of 6.5 Mev gammas.

The results of an adjustment of the type described above are shown in Table II and are plotted for convenience in Fig. 9. Measurements were taken at 8 intervals of 100 volts starting at 2000 volts. The tube saturation voltage was 2700 volts; at this point the 4.43 Mev gammas had a pulse height of 60 volts. Operating voltage was set at about

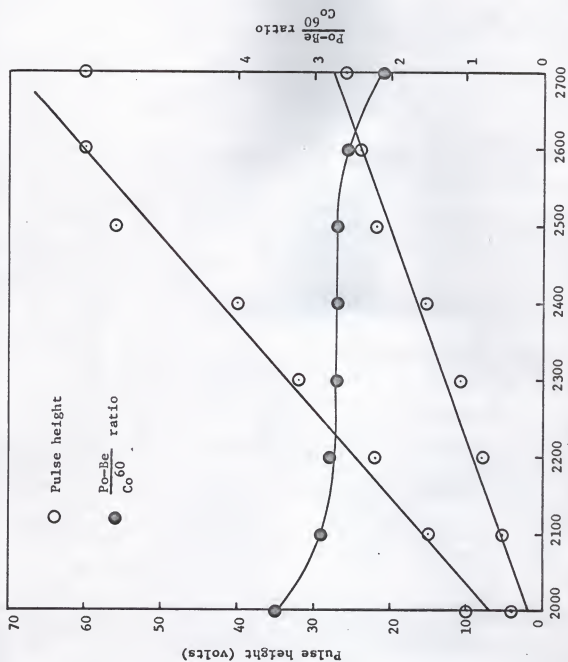


Figure 9. Pulse heights from Po-Be and Co60 gamma-rays vs. photomultiplier tube voltage

2300 volts where the pulse height of the 4.43 Mev gammas was 32 volts.

Table II

Optimum Photomultiplier Voltage Determination

Photomultiplier	Co^{60}	Pulse Height	Po-Be	$\frac{\text{Po-Be}}{\text{Co}^{60}}$
2000 volts	10 volts		4 volts	2.5
2100	15		5.5	2.73
2200	22		8.0	2.75
2300	32		11.0	2.9
2400	40		15.0	2.67
2500	56		22.0	2.54
2600	60		24.0	2.5
2700	60		26.0	2.3

The second adjustment to be made is in the resistance potentiometer grid of the photomultiplier tube. This potentiometer optimizes the multiplication process of the photomultiplier; it is adjusted using the multichannel analyzer to determine the total number of counts recorded at a given potentiometer setting. The equipment is turned on with the high voltage at 2300 volts and given 4 to 5 hours to warm up. The potentiometer is then turned to the point of minimum resistance and a Po-Be source is placed by the detector. Finally the potentiometer is adjusted for optimum counting by setting it at the position that yields

the maximum number of neutron counts.

The third adjustment is the resistance potentiometer at the summing network. This potentiometer adjusts the height of the positive pulses from the 14th phototube dynode to effectively eliminate gamma ray pulses. It is not necessary for all of the gamma ray pulse to be removed at this point; the baseline of the modified A8 amplifier can be raised to eliminate pulses that have been partially canceled out. Accordingly, the adjustment of the summing network resistance potentiometer is made in conjunction with the adjustment of the pulse height selector (Phs) on the modified A8 amplifier.

There are three objectives to meet through these latter two adjustments, namely

1. maintenance of a 1000:1 gamma ray rejection ratio
2. acceptance of neutron pulses down to approximately 0.5 Mev
3. detection of the highest possible number of neutron counts.

Adjusting the two circuits to maintain the above conditions is accomplished by placing a Co^{60} source near the detector so that the dose rate at the detector is 2.5 to 3 mr/hr. The resistance potentiometer is adjusted to an arbitrary position and the Phs of the Mod. A8 amplifier is raised until a gamma ray rejection ratio of 1000:1 is noted. Gamma rejection ratios are measured with the multichannel analyzer; counts are recorded for a period of time in both the anti-coincidence and coincidence modes. The ratio of total counts from the anti-coincidence run to the total counts in the coincidence run is the gamma rejection ratio. Rejection ratios are measured at two linear amplifier gains: a

high gain with "1 cobalt" in channel 200, and a low gain with "1 cobalt" in channel 20.

The next step is to replace the Co^{60} with a Po-Be source and count for a period of time with the multichannel analyzer in the coincidence mode. Particular attention is given to the shape of the spectrum, noting the channel where the peak occurs. To insure detection of neutrons with energies as low as 0.5 Mev, this peak must be in the 10 to 20 channel range during high gain operation. Spectrum distortion can be checked at the low gain; a hump in the trailing edge of the spectrum will occur if the resistance of the potentiometer is too high or if the Phs setting is too low. Proper settings of the resistance potentiometer and the Phs are those that yield a Po-Be spectrum peak in the lowest possible channel without distortion.

An example of this type of adjustment is shown in Table III for phototube voltages of 2300 and 2400 volts. The higher voltage results in settings that yield a Po-Be spectrum peak in a lower channel; however operating at this voltage runs the risk of phototube saturation.

Table III

Modifier A8 and Forte Resistance Potentiometer Settings

Voltage	Mod. A8 Phs		Po-Be Peak Channel	Resistance Potentiometer Turns out from full in
	High Gain	Low Gain		
2300	4.80	5.65	35	12 1/8
2400	6.00	--	27	12 1/8

Adjusting the Linear Amplifiers and the Multichannel Analyzer

The signal from the Modified A8 amplifier is used as a gating pulse input to the multichannel analyzer for coincidence requirements. It is necessary, however, that four pulse conditions be satisfied to meet the input specifications of the multichannel analyzer and still provide the best possible coincidence efficiency. The pulse must be positive, have a height of about 8 to 10 volts, have a rise and fall time of approximately 0.3 microseconds, and be relatively wide. Amplifier modifications provide for two Phs outputs, one negative and the other positive to achieve this; the fine gain control has been removed from the modified system.

Multichannel analyzer (abbreviated MCA) gating requirements can be met by operating the Modified A8 amplifier at a gain of 2 and by using the positive Phs output. The negative Phs output is useful in adjusting the system.

Amplified output from the conventional linear amplifier is checked for linearity using a precision pulser and an oscilloscope. Heights of input and output pulses are measured on the oscilloscope at a particular amplifier gain. The results of a measurement of this type are plotted in Fig. 10; it can be determined that the amplifier is linear within 1.5%.

It is necessary to operate the conventional linear amplifier at both a low and a high gain if the entire range of neutron energies from 0.5 to 14 Mev is to be studied. The high gain setting is so chosen that 1 cobalt is located in channel 200; low gain is set at one-tenth of the high gain, in order that 1 cobalt is placed approximately in channel 20.

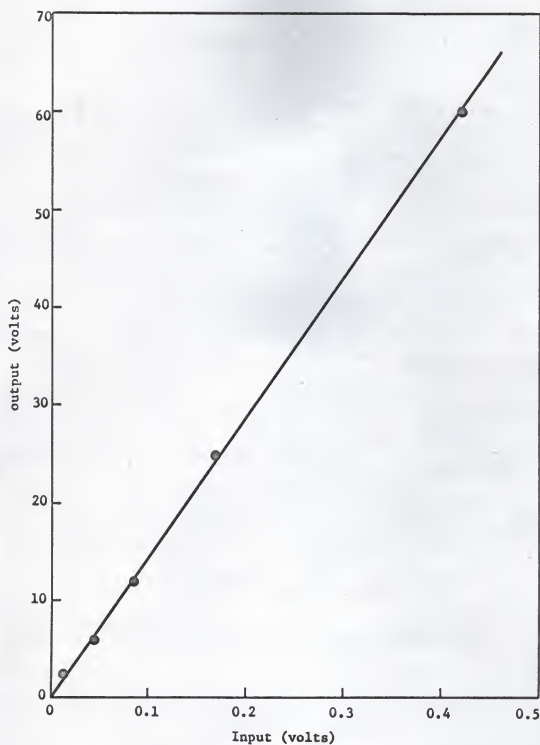


Figure 10. Test of amplifier linearity

High and low gain adjustments are made by feeding a pulse into the linear amplifier with a precision pulser and noting the multichannel analyzer (MCA) channel corresponding to this pulse. For a factor of 10 change in gain adjustment, gain settings on the linear amplifier are adjusted until the pulse is being stored in the appropriate channel, i.e. displaced a factor of 10 from the previous setting.

The only adjustment made on the MCA is the baseline setting; it is set so that a plot of pulse height vs. channel number will have channel zero equal to zero volts. This operation is also carried out using the precision pulser. The pulser output is adjusted until the pulse shape resembles as closely as possible the neutron pulse shapes being analyzed. This pulse is led to the linear amplifier, and then to the high level input of the MCA. The gain on the linear amplifier is adjusted to place the pulses in channel 250. The pulse magnitude is then reduced by a factor of 10; the resulting pulses must fall in channel 25 if the plot of input pulse height vs. channel number is to go through zero. This adjustment is checked at regular intervals to prevent zero drift.

A final check on the conventional linear amplifier and MCA adjustments is made with a Co^{60} source. The amplifier is adjusted to the high gain setting and a Co^{60} source is counted for a period of time with the MCA in anti-coincidence mode. The run is repeated at the low gain setting for the same counting period; gain adjustments are made with the precision pulser as described above. The high gain output is then plotted vs channel number. The low gain output is plotted on the same scale with channel 1 as channel 10, channel 2 as channel 20, etc.,

and with the number of counts in a given channel reduced by a factor of 10. The two plots should fall approximately on one another if all adjustments have been made correctly. If either the gain or baseline settings are not properly adjusted, the plots will not coincide.

Adjusting the Variable Delay

A certain amount of delay is required in the linear amplifier output led to the MCA if the gating input is to be properly timed with respect to this linear amplifier signal. MCA specifications show that it is necessary that the gating input pulse precede the pulse being analyzed by a few tenths of a microsecond. A trial and error procedure is used to determine the proper delay as an alternate to an exact direct measurement.

The proper delay is determined by counting a Po-Be neutron source at the two linear amplifier gain settings with an arbitrary amount of delay in the line between the MCA and the linear amplifier, and the MCA in the coincidence mode. These data are plotted on the gain vs channel number plot described above. If the plots fall on each other, the proper delay is in the line. If not, a new delay setting is tried in the manner noted above until a proper setting is achieved. The proper delay for this work is 2.0 microseconds.

Procedure for Taking Data

Two sources of neutrons, including Po-Be and reactor neutrons, are analyzed in each experiment. The Po-Be neutron source is used to adjust

the equipment as described above. Also, since the Po-Be neutron spectrum has been determined previously by other workers, this spectrum is determined first and used to check the reliability of the counting system.

The procedure used in determining Po-Be data begins with an adjustment of the linear amplifier gain to place 1 cobalt in about channel 200. The source is then placed near the detector and counted long enough to get good counting statistics. At the end of this time the gain is reduced by a factor of 10. The neutron source is not moved during this time; the source is then counted for the same length of time used in the high gain determinations.

The procedure for taking the reactor neutron spectrum data is similar to that used for Po-Be except that the detector is placed in front of the beam port with the collimator in place. The detector is placed 8 feet from the end of the collimator to insure that the beam is spread enough to irradiate the detector uniformly and also to reduce gamma-ray background. A Co^{60} spectrum can be taken with the detector in front of the beam port and with the reactor in operation if the lead shutter in front of the port is closed to cut off reactor neutrons and gamma-rays.

DISCUSSION AND RESULTS

Neutron Spectrum Unfolding Tests

The response functions for monoenergetic neutrons are relatively smooth as compared to the photopeaks present in the response functions for monoenergetic gamma rays. For this reason complex neutron spectrum unfolding using a least squares technique might be more difficult than in the gamma-ray case.

Originally designed for gamma spectrum unfolding, the unfolding method described in the preceding section was tested for its applicability to neutron spectrum unfolding. The response functions used for analyzing the low gain data were combined in two different groups and used as data to test the low gain unfolding code. In the first case the 9th and 10th response functions, corresponding to 5.97 and 8.12 Mev neutrons, respectively, were multiplied by 10^4 and added together to form a "complex spectrum". The 9th and 10th response functions were chosen because they were quite similar; this similarity made them the hardest to unfold from a complex spectrum.

The unfolding code successfully eliminated the 1st eight neutron energies (see Table IV), but could not entirely eliminate the 12th energy. However, the calculated magnitudes of the 9th and 10th energies matched the actual quantities within 0.84×10^{-4} and 6.58×10^{-4} %, respectively.

The second low gain test spectrum included a combination of the 1st 11 response functions, each multiplied by 10^4 . The resulting complex spectrum was analyzed from channel 9 to channel 102; this approximated

Table IV

Low Gain Test Spectrum Containing Two Neutron Energies

N	E(Mev)	Amount Present in Complex Spectrum	Calculated Amount From Unfolding Code	Error in Calculated Amount
1	.335	0.0	0.0	--
2	.6	0.0	0.0	--
3	.946	0.0	0.0	--
4	1.25	0.0	0.0	--
5	1.56	0.0	0.0	--
6	1.91	0.0	0.0	--
7	2.98	0.0	0.0	--
8	3.96	0.0	0.0	--
9	5.97	1.0×10^4	9.916×10^3	0.84×10^2
10	8.12	1.0×10^4	9.342×10^3	6.58×10^2
11	11.0	0.0	0.0	--
12	14.4	0.0	1.402×10^3	1.402×10^3

actual conditions encountered in this research. In analyzing actual complex spectra the lower channel limit is at the peak of the complex spectra and the upper channel limit is the channel where the spectra first go to zero.

The results of the second test spectrum analysis are shown in Table V. The first 4 energies were eliminated as expected since their response fell below channel 9, which was the lowest channel number analyzed. The

Table V

Low Gain Test Spectrum Containing Eleven Neutron Energies

N	E(Mev)	Amount Present in Complex Spectrum	Calculated Amount From Unfolding Code	Error in Calculated Amount
1	.335	1.0×10^4	0.0	--
2	.6	1.0×10^4	0.0	--
3	.946	1.0×10^4	0.0	--
4	1.25	1.0×10^4	0.0	--
5	1.56	1.0×10^4	2.374×10^5	22.74×10^4
6	1.91	1.0×10^4	9.361×10^3	6.39×10^2
7	2.98	1.0×10^4	9.96×10^3	0.37×10^2
8	3.96	1.0×10^4	9.975×10^3	0.25×10^2
9	5.97	1.0×10^4	1.000×10^4	0.0
10	8.12	1.0×10^4	1.004×10^4	0.04×10^2
11	11.0	1.0×10^4	9.543×10^3	4.57×10^2
12	14.4	0.0	6.58×10^2	6.58×10^2

magnitude of the 5th energy present was too large. This can be explained by the fact that the response for the 5th energy ends in the 9th channel. Thus, only one channel (channel 9) of the analyzed data contained a response for the 5th energy; an accurate determination of the amount of the 5th energy present would not be possible with just one channel. As in the first test, the 12th energy was not entirely eliminated.

The above low gain unfolding tests indicated that little faith can

be placed in the accuracy of the results obtained for both the 12th and the lowest accepted energy. However, the tests show that results for intermediate energies should be accurate within approximately .0007% (the largest single error in the calculated amounts).

A test of the unfolding technique at the high gain was performed by multiplying all 12 neutron energy responses by 10^4 and combining to form a complex spectrum. The unfolded results are shown in Table VI and were obtained by analyzing from channel 22 to channel 200. The large

Table VI

High Gain Test Spectrum Containing Twelve Neutron Energies

N	E(Mev)	Amount Present in Complex Spectrum	Calculated Amount From Unfolding Code	Error in Calculated Amount
1	.335	1.0×10^4	1.911×10^6	190.1×10^4
2	.6	1.0×10^4	8.327×10^3	16.673×10^2
3	.946	1.0×10^4	1.003×10^4	$.03 \times 10^2$
4	1.25	1.0×10^4	9.995×10^3	$.05 \times 10^2$
5	1.56	1.0×10^4	1.001×10^4	$.01 \times 10^2$
6	1.91	1.0×10^4	1.000×10^4	0.0
7	2.98	1.0×10^4	9.998×10^3	$.02 \times 10^2$
8	3.96	1.0×10^4	9.983×10^3	$.17 \times 10^2$
9	5.97	1.0×10^4	1.003×10^4	$.03 \times 10^2$
10	8.12	1.0×10^4	1.016×10^4	$.16 \times 10^2$
11	11.0	1.0×10^4	9.749×10^3	2.51×10^2
12	14.4	1.0×10^4	0.984×10^3	$.16 \times 10^2$

error in the first two energies can be attributed to the channel 22 cut-off; only a very small portion of the response for these two energies is seen by the computer.

Po-Be Neutron Spectra

A Po-Be neutron spectrum was recorded at a high and a low gain; these spectra were then analyzed with the previously described unfolding code. The low gain complex spectrum is shown in Figs. 11 and 12 and the high gain complex spectrum is shown in Fig. 13.

The Po-Be low gain complex spectrum was characterized by a "peaking" effect in the channel 70 to 100 region. A peak was recorded in this region interrupting a spectrum that, otherwise, descended smoothly from approximately 15,200 counts in channel 4 to zero counts in channel 135.

This peaking effect occurred after raising the phototube operating voltage to 2300 volts and after adjusting the resistance potentiometer of the Forte circuit. These adjustments were made in an attempt to shift the high gain Po-Be spectrum peak to the lowest possible channel and, thus, detect neutrons with energies as low as 0.5 Mev.

The assumed probable cause for this peaking effect was the detection of high energy gamma-ray counts. A Co^{60} source was counted in conjunction with the Po-Be source to test this assumption; the magnitude of the peak increased sharply while the rest of the spectrum was unchanged. Apparently, at a phototube voltage of 2300 volts and at certain potentiometer settings, Forte circuit gamma-ray discriminating capabilities are impaired, allowing gamma-ray activity to be recorded.

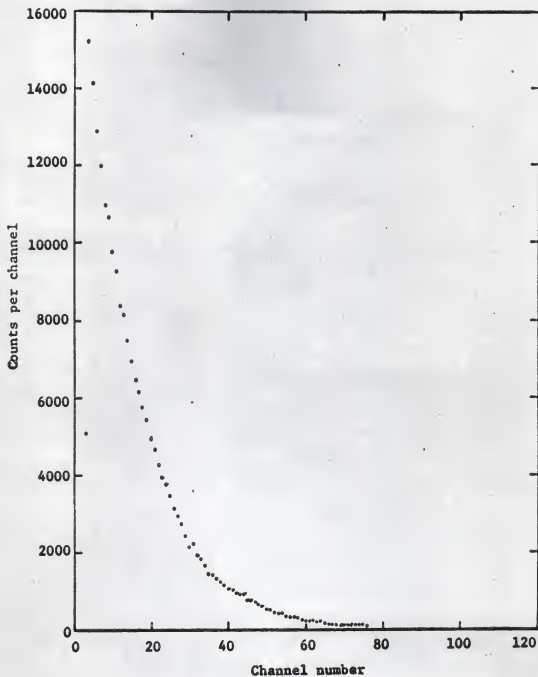


Figure 11. Low gain Po-Ba complex neutron spectrum

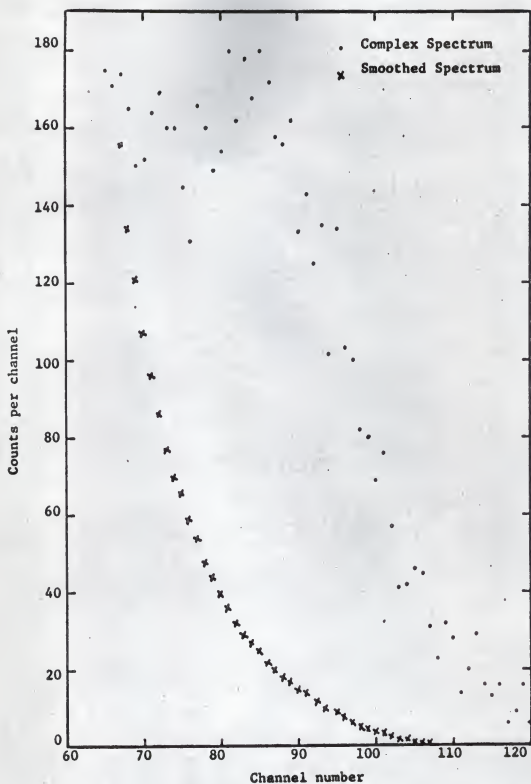


Figure 12. Low gain Po-Be complex and smoothed spectra

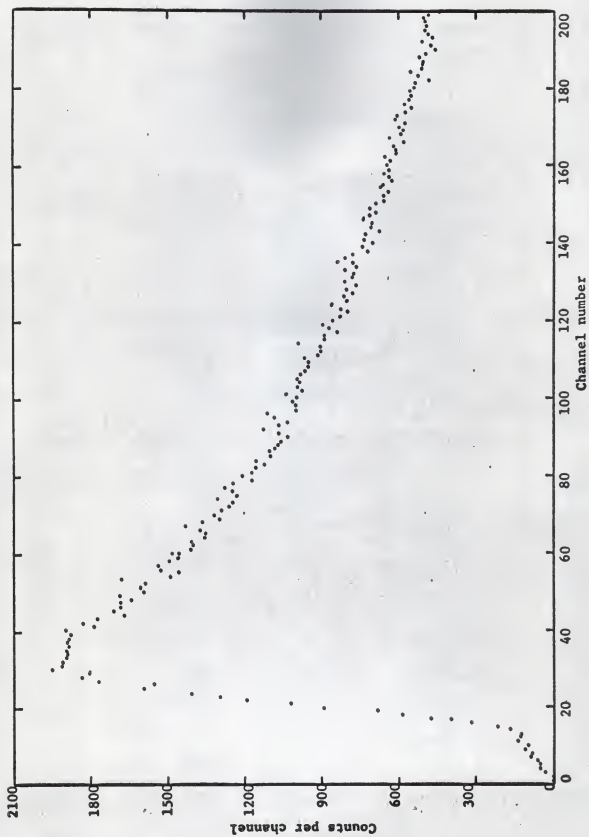


Figure 13. High gain Po-Be complex neutron spectrum

Data were recorded at these "overload conditions" with a sacrifice in accuracy at the higher channels to describe as much as possible of the low energy neutron spectrum. The spectrum was smoothed (see Fig. 12) in the peaking region with a "non-peaked" Po-Be spectrum which had been recorded at a lower phototube voltage and a different potentiometer setting.

The Po-Be low gain spectrum was compared with a Po-Be spectrum obtained with the ORNL NE-213 spectrometer system (see Fig. 14). The ORNL spectrum was normalized to the spectrum measured here at channel 10. Remaining points were within at least 5% of the ORNL spectrum, indicating good similarity between the two systems at high neutron energies (low gain).

An unfolded Po-Be spectrum (see Fig. 15 for results and theoretical Po-Be spectrum of Whitmore and Baker (23)) was obtained from the low and high gain spectra. Unfolding techniques for the low gain spectrum were completed without difficulty; however, a satisfactory unfolded high gain spectrum was not obtained. When analyzing the high gain spectrum, the unfolded least squares solution retained some energy values (plotted in Fig. 15), but rejected intermediate values; this is not acceptable since Po-Be is known to have a continuous neutron energy spectrum. An attempt was made to unfold the high gain spectrum using 22 monoenergetic neutron spectra rather than 12; the additional 10 monoenergetic spectra were obtained by extrapolating between the 12 available spectra. This attempt was also unsuccessful.

The failure to unfold the high gain spectrum is concluded to result from a small difference in the monoenergetic neutron response of the

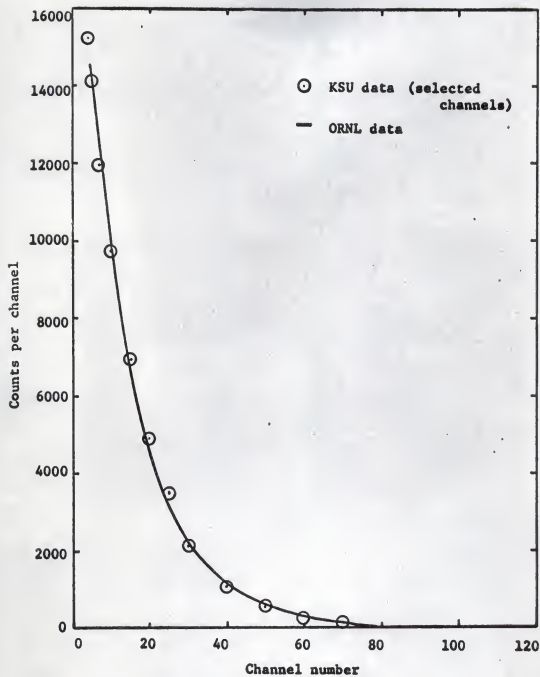


Figure 14. Comparison of KSU Po-Be spectrum to ORNL Po-Be spectrum

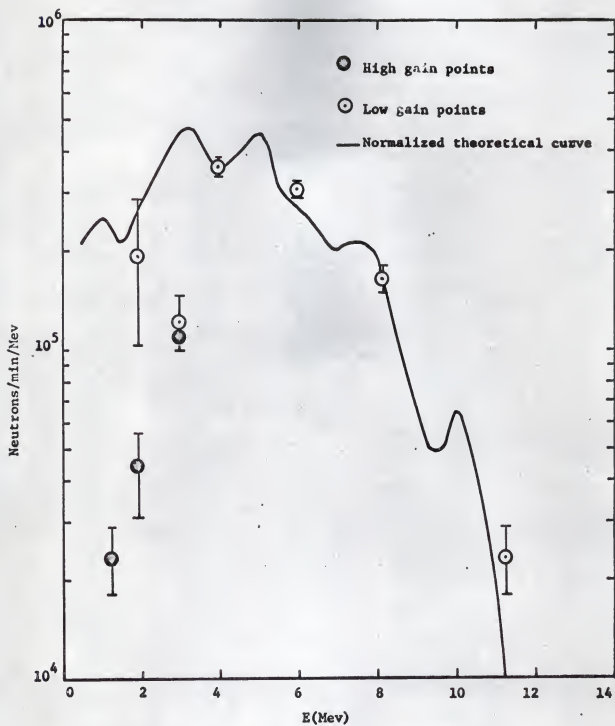


Figure 15. Unfolded Po-Be spectrum with theoretical curve by Whitmore and Baker (23)

system used in this work compared with response of the ORNL system. Apparently, no gross differences exist since the low gain spectrum match the ORNL low gain spectrum within at least 5% (see Fig. 14). The difference is most probably in the resolution of the systems; difference in resolution would not be apparent at the low gain, but could be significant in the high gain (high spectrum resolution region).

Burrus and Verbinski (6) determined the "fractional resolution" of the ORNL system by "dividing the difference in pulse height between the 88% point and the 12% point of the upper edge of the pulse-height distribution (in suitable pulse-height units) by the pulse height of the 50% point". A comparable resolution measurement with the KSU system is not possible since the peak of any one neutron spectrum (lower channel cut-off point) for this system falls in a different channel than that of the ORNL system. Identical spectra for the two systems will have peaks of different magnitude due to this difference in lower channel cut-off; this prevents a comparison of resolution as determined by the ORNL method.

Reactor Neutron Spectra

Reactor neutron spectra were recorded at low and high gains for reactor power levels of 1 and 5 watts (see Figs. 16 to 22). The detector assembly was positioned 8 ft. from the end of the collimator at the fast beam port as discussed in a preceding section.

As noted with the Po-Be spectra, the low gain reactor neutron spectra were unfolded with reasonable results; attempts to unfold the high gain neutron spectra were again unsuccessful. Gamma peaking in the low gain

data was smoothed with the use of spectra recorded in the absence of peak-
ing. Results of the low gain unfolding are shown in Figs. 23 and 24 with
the curve predicted by Joanou and Dudek (12); several high gain points
are also shown.

One high gain spectrum was recorded at a phototube voltage of 2400
volts. The higher phototube voltage made it possible to detect neutrons
of lower energy; but no significant improvement in the unfolded results
was obtained.

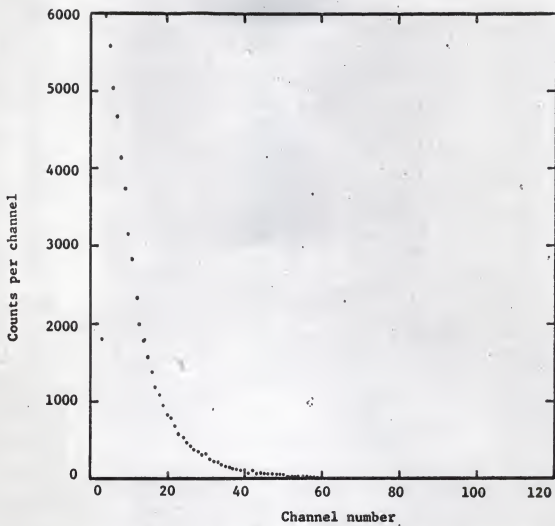


Figure 16. One watt low gain reactor complex spectrum

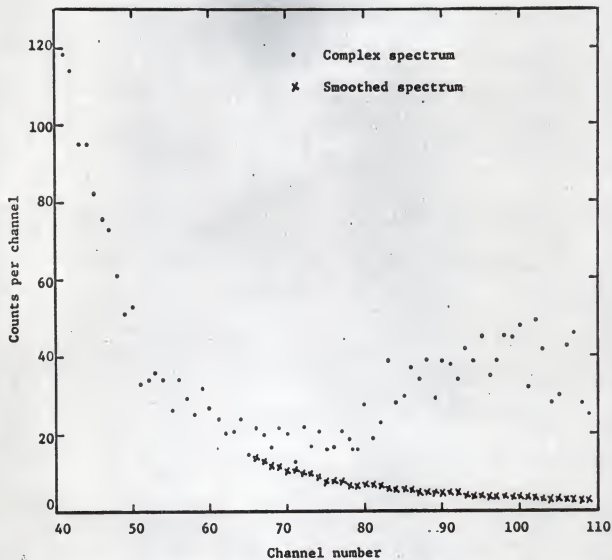


Figure 17. One watt low gain reactor complex and smoothed spectra

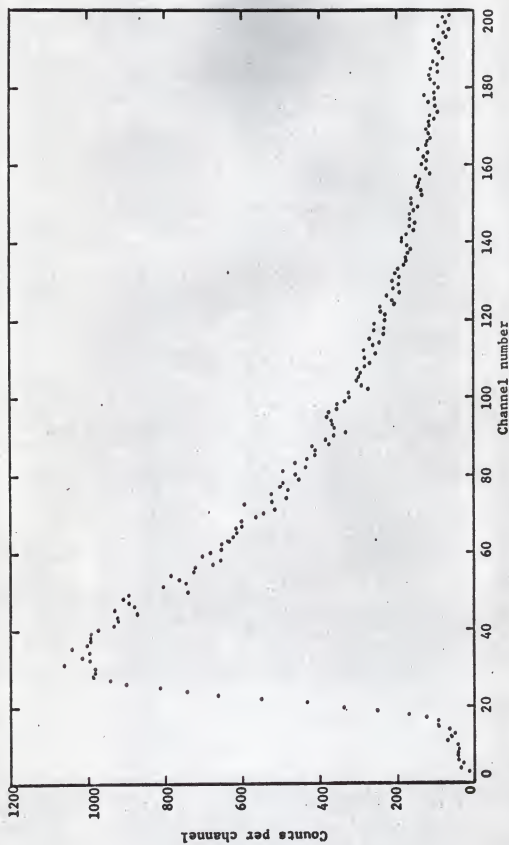


Figure 18. One watt high gain reactor complex spectrum

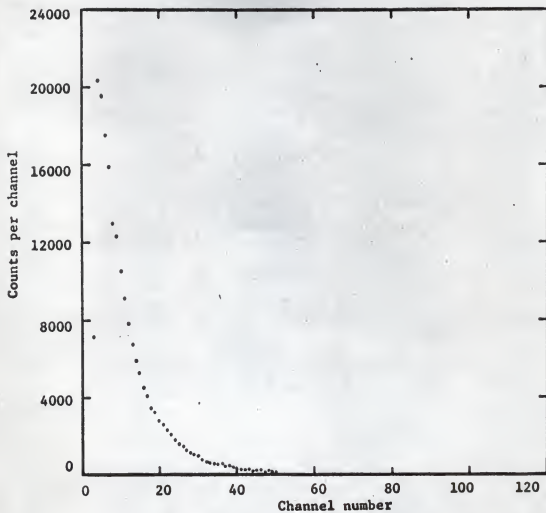


Figure 19. Five watt low gain reactor complex spectrum

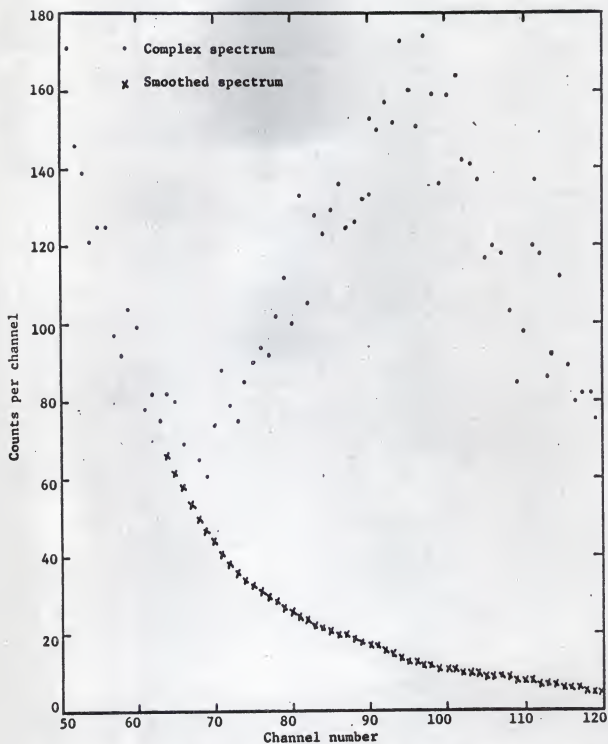


Figure 20. Five watt low gain reactor complex and smoothed spectra

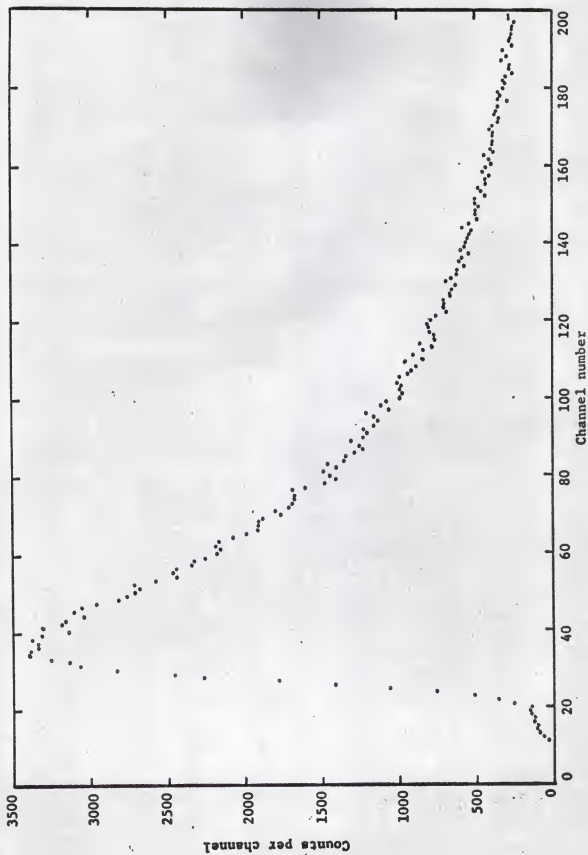


Figure 21. Five watt high gain reactor complex spectrum

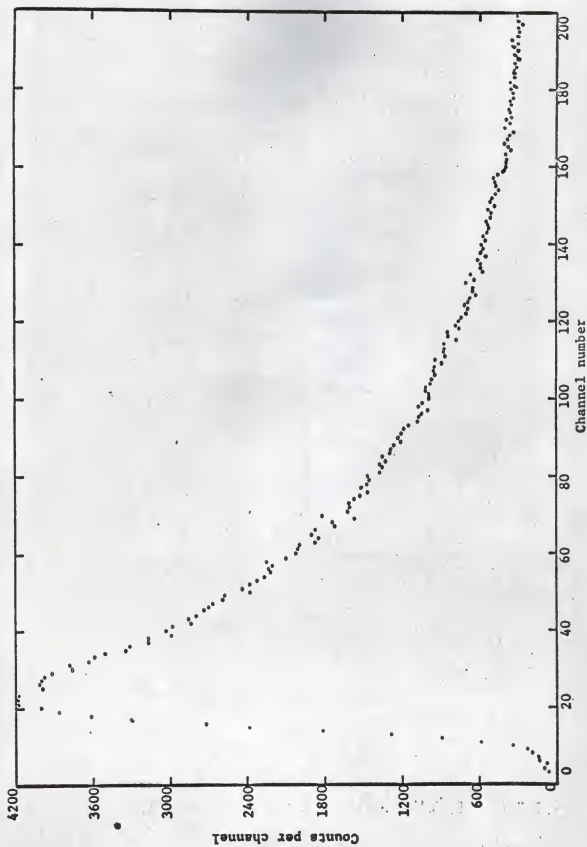


Figure 22. Five watt high gain reactor complex spectrum at 2400 photomultiplier volts

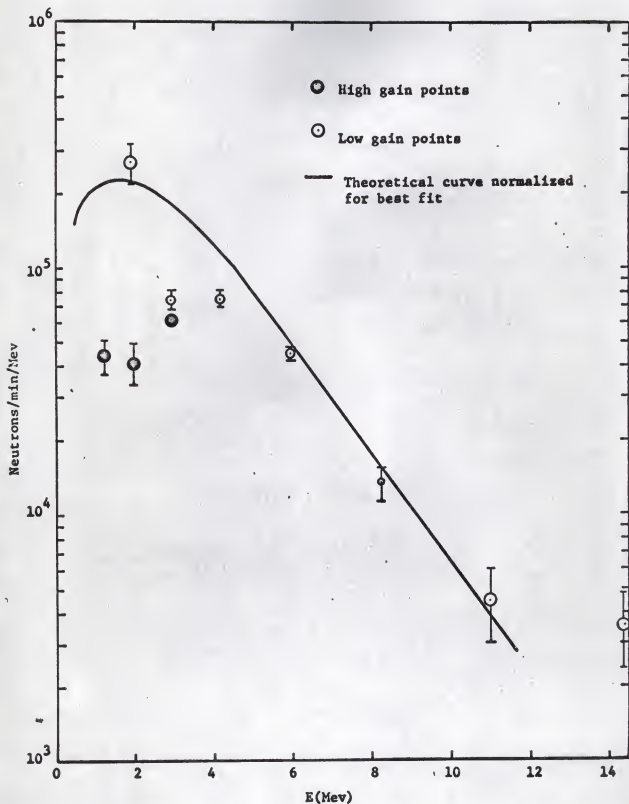


Figure 23. Unfolded 1 watt reactor neutron spectrum with theoretical curve of Joanou and Dudek (12)

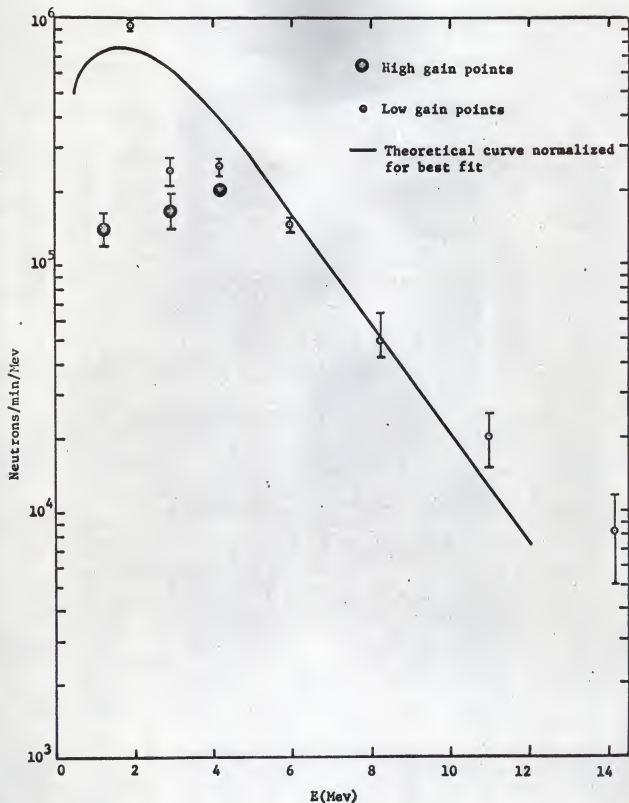


Figure 24. Unfolded 5 watt reactor neutron spectrum with theoretical curve by Joanou and Dudek (12)

CONCLUSIONS

Response of the NE-213 spectrometer system used in this work to neutrons in the 2 to 14 Mev energy range (recorded at low gain) was evidently very similar to the system at ORNL. Low gain Po-Be complex spectra were nearly identical (within at least 5%) to ORNL Po-Be complex spectra; the ORNL data have been successfully unfolded and agree with the generally accepted spectrum of Whitmore and Baker (23) (see Appendix D).

Response of the system to low energy neutrons was improper. No gross malfunction is suspected to exist since this would be evident in the low gain data. The error is probably in the resolution of the system; resolution errors would be most significant for the high gain spectrum when the spectrum is spread out in fine detail.

Poor resolution may result from a lack of proper optical coupling between the scintillator bottle and photomultiplier tube. The scintillator bottle is joined to the phototube with Dow Corning 10^6 centistokes silicone compound. All streaks and air bubbles in the grease must be eliminated for proper coupling and good resolution. Since, as noted earlier, the bottle is coated with a white reflector paint, it was not possible to determine directly if all streaks and bubbles were eliminated during the coupling procedure.

The NE-213 spectrometer system did not detect neutrons in the 0.5 to 2.0 Mev energy range without a peaking effect in the low gain spectra. The peaking effect was not apparent when detecting neutrons with energies from 1 to 14 Mev. However, as adjustments were made in phototube voltage

and Forte circuit resistance potentiometer settings to extend the detectable neutron energies to 0.5 Mev, peaking in the low gain spectra was noticed. Evidently, the phototube and potentiometer adjustments caused the gamma discriminator circuit to fail and higher energy gamma rays were detected and counted.

There were no obvious explanations for the failure of the gamma-ray discriminating circuit. The failure may be caused by a poor electronic component in the circuit or by an improper Forte circuit adjustment. In any case, the failure did not completely invalidate the results of this work; the peaking effect could be eliminated with the aid of "non-peaked" spectra.

SUGGESTIONS FOR FURTHER STUDY

Neutron energy resolution of the NE-213 neutron spectrometer system used in this work can be improved by replacing the white reflector paint on the scintillator bottle with aluminum foil (shiny side in). A similar substitution at ORNL (6) reduced the resolution from 11 to 6.5%. Improved resolution may make it possible to unfold high gain complex neutron spectra.

Electronic components of the pulse shape discriminator circuit should be thoroughly examined for defective parts. Operation at high voltages may require that certain components be shielded or relocated to prevent interference with other components.

The response of the system used in this work to monoenergetic neutrons should be checked by exposing the detector to monoenergetic neutrons produced with the Kansas State University Nuclear Engineering heavy particle accelerator. Several different neutron energies are available from this accelerator. Using these monoenergetic spectra, factors can be determined to correct the monoenergetic ORNL response functions. Further, it would be desirable to develop a complete library of experimentally determined monoenergetic responses. These responses would be characteristic of the KSU system and would be expected to give better results than can be obtained with the ORNL system characteristic functions.

Further applications of the NE-213 neutron spectrometer used in this work are numerous. Fellow student, Capt. James Kapitzke, is presently measuring fast neutron dose albedos using this system. Gale Simons, Grad-

uate U.S.A.E.C. Fellow, has proposed the use of this system for experimentally determining monoenergetic neutron cross sections.

ACKNOWLEDGMENT

The author wishes to express his gratitude to Dr. Walter Meyer under whose direction this study was accomplished. Special thanks must also go to Dr. C. E. Clifford of Oak Ridge National Laboratory who suggested the study. Sincere appreciation is also extended to Dr. W. R. Kimel, Head of the Kansas State University Department of Nuclear Engineering, for his encouragement and coordinating efforts with ORNL, and to the Kansas State University Engineering Experiment Station for their financial support. Recognition must also be given to fellow students, Capt. James Kapitzke and Gale Simons, Graduate U.S.A.E.C. Fellow, for their contributions, and to Dean Eckhoff, Nuclear Engineering staff member, for his assistance with the unfolding code.

LITERATURE CITED

1. Adelson, Harold E., Hoyt A. Bostick, Burton J. Moyer, and Charles N. Waddell
Use of the Four-Inch Liquid Hydrogen Bubble Chamber as a Fast-Neutron Spectrometer. *Rev. Sci. Inst.*, 31: 1 (1960).
2. Allred, J. C., A. H. Armstrong and L. Rosen
The Interaction of 14-Mev Neutrons with Protons and Deuterons. *Phys. Rev.*, 91: 90 (1953).
3. Batchelor, R., R. Aves and T. H. R. Skyrme
Helium-3 Filled Proportional Counter for Neutron Spectroscopy. *Rev. Sci. Inst.*, 26: 1037 (1955).
4. Bonner, T. W., R. A. Ferrell and M. C. Rinehart
A Study of the Spectrum of the Neutrons of Low Energy from the Fission of U^{235} . *Phys. Rev.*, 87: 1032 (1952).
5. Broek, H. W., and C. E. Anderson
The Stilbene Scintillation Crystal as a Spectrometer for Continuous Fast-Neutron Spectra. *Rev. Sci. Inst.*, 31: 1063 (1960).
6. Burrus, W. R. and V. V. Verbinski
Recent Developments in the Proton-Recoil Scintillation Neutron Spectrometer. *Trans. Am. Nucl. Soc.*, 7: 373-4 (1964).
7. Draper, J. E.
A Fast Neutron-Scintillation Spectrometer. *Rev. Sci. Inst.*, 25: 558 (1954).
8. Eckhoff, N. D. and T. R. Hill
Personal Communication. Department of Nuclear Engineering, Kansas State University, Manhattan, Kansas.
9. Eliot, E. A., D. Hicks, L. E. Beghian and H. Halban
Inelastic Scattering of Neutrons. *Phys. Rev.*, 94: 144 (1954).
10. Glasstone, Samuel and Milton C. Edlund
Nuclear Reactor Theory. D. Van Nostrand Company, New York (1962).
11. Goldstein, Herbert
The Attenuation of Gamma Rays and Neutrons in Reactor Shields. Nuclear Development Corporation of America, New York (1957).
12. Joanou, G. D. and J. S. Dudek
Gam-1: A Consistent P_1 Multigroup Code for the Calculation of Fast Neutron Spectra and Multigroup Constants. GA-1850.

13. Johnson, C. H. and C. C. Trail
Proton-Recoil Neutron Spectrometer. Rev. Sci. Inst., 27: 468 (1956).
14. Kaplan, Irving
Nuclear Physics. Addison-Wesley Publishing Company, Inc., Reading, Massachusetts (1963).
15. Murray, R. B.
Use of $\text{Li}^{6}\text{I}(\text{Eu})$ as a Scintillation Detector and Spectrometer for Fast Neutrons. Nuc. Inst. Meth., 2: 237 (1958).
16. Neilson, G. C. and D. B. James
Time of Flight Spectrometer for Fast Neutrons. Rev. Sci. Inst., 26: 1018 (1955).
17. Poole, M. J.
Neutron Flux and Spectrum Measurement. Proc. Phys. Soc. (London), A65: 453 (1952).
18. Price, William J.
Nuclear Radiation Detection. McGraw-Hill, New York (1964).
19. Rockwell, Theodore, ed.
Reactor Shielding Design Manual. D. Van Nostrand Company, Princeton, N. J. (1956).
20. Scintillator Catalogue. Nuclear Enterprises, Ltd. Cleveland, Ohio.
21. Trombka, J. I.
Least-Squares Analysis of Gamma-Ray Pulse-Height Spectra. NAS-NS-3107.
22. Verbinski, V. V., J. C. Courtney, W. R. Burrus and T. A. Love
The Response of Some Organic Scintillators to Fast Neutrons. ORNL-P-993.
23. Whitmore, B. G. and W. B. Baker
The Energy Spectrum of Neutrons from a Po-Be Source. Phys. Rev., 78: 799 (1950).

APPENDICES

APPENDIX A

Absolute Differential Efficiency as a Function of Light
Output (in "Cobalt" Units) for Plane Parallel Monoenergetic
Neutrons Perpendicular to Axes of 2" x 2" diameter Cylinder
of NE-213 Scintillator

PULSE HEIGHT	0.335 MEV	0.6 MEV	0.946 MEV	1.25 MEV	1.56 MEV	1.91 MEV
.0100	18.832371	8.926455	5.377247	3.967391	3.425863	2.661284
.0105	19.089036	8.884234	5.319968	3.869448	3.311990	2.685975
.0110	19.371890	8.025534	5.249994	3.772750	3.204328	2.535228
.0115	19.716326	8.767020	5.176998	3.682205	3.105990	2.408003
.0120	20.145219	8.722239	5.109389	3.602102	3.019674	2.303191
.0126	20.663601	8.698753	5.052380	3.534875	2.946667	2.215034
.0132	21.258274	8.696790	5.007051	3.480439	2.886210	2.152693
.0138	21.902869	8.710398	4.970854	3.436410	2.835757	2.100448
.0145	22.567061	8.730377	4.939068	3.399116	2.791682	2.058211
.0151	23.224801	8.747823	4.906694	3.364775	2.750312	2.022195
.0158	23.859646	8.757074	4.870090	3.330581	2.708813	1.989496
.0166	24.463748	8.757195	4.827864	3.295247	2.665692	1.958371
.0174	25.031565	8.751853	4.750728	3.258937	2.620783	1.928155
.0182	25.550417	8.747964	4.730870	3.222745	2.574850	1.898913
.0191	25.990642	8.753667	4.650659	3.157873	2.528954	1.870919
.0200	26.300681	8.776755	4.631749	3.155005	2.483377	1.844238
.0209	26.410219	8.824010	4.584743	3.124129	2.439928	1.818595
.0219	26.239648	8.901148	4.539353	3.094618	2.396956	1.793399
.0229	25.715206	9.013055	4.494890	3.065575	2.354588	1.767975
.0240	24.785860	9.163935	4.450799	3.036274	2.312571	1.741803
.0251	23.436189	9.356706	4.407102	3.006325	2.270968	1.714680
.0263	21.693169	9.592261	4.364405	2.975672	2.230175	1.686728
.0275	19.625241	9.868701	4.323515	2.944456	2.190897	1.658349
.0288	17.331893	10.180451	4.285357	2.912755	2.153873	1.630013
.0302	14.930454	10.518262	4.250803	2.880574	2.119796	1.602186
.0316	12.539898	10.868835	4.220647	2.847843	2.089195	1.575274
.0331	10.266278	11.214167	4.195725	2.814524	2.062310	1.549555
.0347	8.192492	11.550656	4.177005	2.780738	2.039032	1.525183
.0363	6.373177	11.788567	4.165614	2.746800	2.018854	1.502145
.0380	4.334271	11.952865	4.162910	2.713220	2.000917	1.480311

PULSE HEIGHT	0.335 MEV	0.6 MEV	0.946 MEV	1.25 MEV	1.56 MEV	1.91 MEV
•0398	3.576646	11.985937	4.170364	2.680668	1.984056	1.459406
•0417	2.581951	11.852747	4.189566	2.649891	1.967016	1.439084
•0437	1.819370	11.527284	4.222163	2.621718	1.948700	1.419025
•0457	1.251941	10.998336	4.269736	2.596976	1.928399	1.398988
•0479	.841630	10.273583	4.333522	2.576475	1.905742	1.378863
•0501	.552999	9.380111	4.414017	2.560979	1.881135	1.358698
•0525	.352990	8.361304	4.510514	2.551174	1.855291	1.338665
•0550	.223297	7.270679	4.620362	2.547575	1.829161	1.318970
•0575	.137344	6.164701	4.738469	2.550580	1.803782	1.299837
•0603	.082707	5.095549	4.856909	2.560354	1.779984	1.281395
•0631	.048782	4.105717	4.965066	2.576849	1.758328	1.263677
•0661	.028193	3.225002	5.050426	2.599884	1.739110	1.246634
•0692	.015972	2.469767	5.099689	2.629033	1.722412	1.230178
•0724	.000874	1.844221	5.100209	2.663686	1.708264	1.214213
•0759	.004837	1.342898	5.041694	2.702888	1.696758	1.198762
•0794	.002588	.953606	4.916975	2.745131	1.688130	1.183914
•0832	.001359	.660388	4.723403	2.788239	1.682786	1.169893
•0871	.000701	.445991	4.462652	2.829131	1.681222	1.156978
•0912	.000356	.293720	4.140982	2.863873	1.883941	1.145479
•0955	.000177	.188627	3.768244	2.887833	1.691313	1.135643
•1000	.000087	.118120	3.358092	2.896176	1.703515	1.127647
•1047	.000042	.072124	2.926072	2.884310	1.720398	1.121541
•1096	.000020	.042941	2.489087	2.848354	1.741418	1.117303
•1148	.000009	.024930	2.033887	2.785422	1.765517	1.114890
•1202	.000004	.014114	1.665329	2.693655	1.791068	1.114307
•1259	.000002	.007793	1.305861	2.572166	1.815792	1.115665
•1318	.000001	.004197	.993766	2.421102	1.836889	1.119178
•1380	.000000	.002205	.733096	2.241806	1.851211	1.125100
•1445	.000000	.001200	.537395	2.050043	1.852392	1.130858
•1514	.000000	.000657	.398433	1.869666	1.840009	1.133188

PULSE HEIGHT	0.335 MEV	0.6 MEV	0.946 MEV	1.25 MEV	1.56 MEV	1.91 MEV
•1585	•000000	•000252	•257323	1.639770	1.826123	1.145141
•1660	•000000	•000090	•157113	1.397517	1.796834	1.158985
•1738	•000000	•000030	•090223	1.152036	1.750415	1.173659
•1820	•000000	•000009	•048466	•913930	1.685757	1.187479
•1905	•000000	•000003	•024215	•694004	1.602101	1.198227
•1995	•000000	•000001	•011186	•501612	1.498660	1.203364
•2089	•000000	•000000	•004749	•343086	1.374545	1.200439
•2188	•000000	•000000	•001841	•220726	1.229295	1.187548
•2291	•000000	•000000	•000648	•132739	1.064126	1.163660
•2399	•000000	•000000	•000205	•074127	•883568	1.128719
•2512	•000000	•000000	•000058	•038172	•696489	1.083333
•2630	•000000	•000000	•000015	•017992	•515447	1.028009
•2754	•000000	•000000	•000003	•007701	•354067	•962332
•2884	•000000	•000000	•000081	•002968	•223174	•884474
•3020	•000000	•000000	•000000	•001021	•127629	•791730
•3162	•000000	•000000	•000000	•000311	•065494	•682367
•3311	•000000	•000000	•000000	•000083	•029831	•558214
•3467	•000000	•000000	•000000	•000019	•011930	•426525
•3631	•000000	•000000	•000000	•000004	•004144	•299316
•3802	•000000	•000000	•000000	•000001	•001237	•189688
•3981	•000000	•000000	•000000	•000000	•000314	•106789
•4169	•000000	•000000	•000000	•000000	•000067	•052563
•4365	•000000	•000000	•000000	•000000	•000012	•022275
•4571	•000000	•000000	•000000	•000000	•000002	•008006
•4786	•000000	•000000	•000000	•000000	•000000	•002405
•5012	•000000	•000000	•000000	•000000	•000000	•000595
•5248	•000000	•000000	•000000	•000000	•0000 0	•000120
•5495	•000000	•000000	•000000	•000000	•000000	•000019
•5754	•000000	•000000	•000000	•000000	•000000	•000002
•6026	•000000	•000000	•000000	•000000	•000000	•000000

PULSE HEIGHT	2.98 MEV	3.96 MEV	5.97 MEV	8.12 MEV	11.0 MEV	14.4 MEV
.0100	5.052496	5.240069	6.104021	6.019078	4.476133	2.667461
.0105	4.379364	4.963158	5.784702	5.712537	4.335658	2.528069
.0110	3.808562	4.636828	5.403548	5.345988	4.176313	2.398176
.0115	3.325225	4.271771	4.973373	4.932181	4.005106	2.278579
.0120	2.916896	3.882246	4.511459	4.487733	3.829138	2.170081
.0126	2.573126	3.483846	4.036677	4.030640	3.653869	2.072741
.0132	2.284567	3.091448	3.560007	3.577779	3.481882	1.985290
.0138	2.044095	2.717697	3.17785	3.143207	3.312592	1.905149
.0145	1.843627	2.372215	2.700389	2.737316	3.142867	1.828820
.0151	1.677127	2.061361	2.322592	2.366639	2.968260	1.752593
.0158	1.539189	1.788447	1.988278	2.034263	2.784460	1.673262
.0166	1.425319	1.554211	1.698231	1.740604	2.588600	1.588686
.0174	1.331843	1.357369	1.451009	1.484205	2.380061	1.498049
.0182	1.255718	1.195171	1.243446	1.262502	2.160802	1.401819
.0191	1.194271	1.063856	1.071596	1.072405	1.934960	1.301383
.0200	1.145007	.959089	.930814	.910662	1.708150	1.198585
.0209	1.105559	.876335	.816596	.774109	1.486576	1.095358
.0219	1.073710	.811202	.724531	.659766	1.276121	.993368
.0229	1.047502	.759719	.650628	.564876	1.081685	.893917
.0240	1.025328	.718519	.591409	.486902	.906751	.797962
.0251	1.005963	.684931	.543934	.423524	.753272	.706238
.0263	.988508	.656959	.595773	.372607	.621769	.619398
.0275	.972324	.633193	.474946	.332203	.511575	.539111
.0288	.956879	.612675	.449829	.300532	.421156	.463071
.0302	.941731	.594769	.429099	.275995	.348453	.394973
.0316	.926495	.579066	.411690	.257184	.291177	.334426
.0331	.910863	.565286	.396758	.242881	.247038	.281870
.0347	.894613	.553210	.383699	.232055	.213914	.237510
.0363	.877629	.542634	.371914	.223846	.189948	.201285
.0380	.859892	.533332	.361193	.217550	.173585	.172887

PULSE HEIGHT	2.98 MEV	3.96 MEV	5.97 MEV	8.12 MEV	11.0 MEV	14.4 MEV
.0398	.841449	.525049	.351268	.212593	.163564	.151790
.0417	.822404	.517498	.341996	.208513	.158879	.137301
.0437	.802912	.510391	.333252	.204958	.157181	.128608
.0457	.783177	.503454	.325000	.201666	.162395	.124825
.0479	.763435	.496452	.317179	.198458	.162888	.125028
.0501	.743950	.489201	.309742	.195223	.178798	.128301
.0525	.725002	.481587	.302649	.191907	.133778	.128301
.0550	.706830	.473559	.295852	.188484	.203273	.140691
.0575	.689635	.465135	.299309	.184952	.217026	.148411
.0603	.673536	.456389	.282968	.181313	.230987	.156463
.0631	.658570	.447440	.276788	.177563	.244570	.164509
.0661	.644714	.438433	.270735	.173706	.257214	.172312
.0692	.631885	.429504	.264776	.169750	.268389	.179660
.0724	.619983	.420762	.258860	.165719	.277612	.186305
.0759	.608897	.412260	.253056	.161660	.284462	.191912
.0794	.598511	.403992	.247252	.157656	.288609	.196066
.0832	.588701	.395908	.241450	.153772	.289846	.198313
.0871	.579319	.387915	.235615	.150137	.288116	.198250
.0912	.570194	.379930	.229711	.146830	.283527	.195616
.0955	.561147	.371885	.223705	.143911	.276338	.190372
.1000	.552033	.363768	.217593	.141394	.266924	.182745
.1047	.542780	.355621	.211403	.139241	.255723	.173207
.1096	.533448	.347530	.205211	.137360	.243178	.162430
.1148	.524224	.339654	.199122	.135625	.229706	.151194
.1202	.515409	.332117	.193256	.133892	.215675	.140305
.1259	.507332	.325055	.187707	.132030	.201412	.130504
.1318	.500274	.318570	.182523	.129942	.187242	.122406
.1380	.494379	.312715	.177695	.127596	.173489	.116463
.1445	.489074	.307339	.173156	.125009	.161169	.112934
.1514	.483452	.302098	.168848	.122320	.150827	.110992

PULSE HEIGHT	2.98 MEV	3.96 MEV	5.97 MEV	8.12 MEV	11.0 MEV	14.4 MEV
•1585	•479974	•297807	•164539	•119655	•139531	•111052
•1660	•476990	•294044	•160259	•117068	•129632	•113539
•1738	•474080	•290701	•155923	•114760	•121337	•118205
•1820	•470857	•287635	•131509	•112935	•114727	•124624
•1905	•467075	•284691	•147098	•111738	•109716	•132195
•1995	•462703	•281705	•142775	•111192	•106043	•140150
•2089	•457939	•278557	•138796	•111151	•103294	•147582
•2188	•453163	•275170	•135340	•111288	•100953	•153517
•2291	•448818	•271570	•132591	•111164	•098459	•157041
•2399	•445320	•267827	•130539	•110348	•095289	•157479
•2512	•442951	•264049	•129125	•108574	•091046	•154562
•2630	•441792	•260336	•128096	•105851	•085552	•148512
•2754	•441703	•256801	•127121	•102471	•078933	•140000
•2884	•442349	•253606	•125869	•098901	•071630	•129964
•3020	•443324	•251019	•124131	•095616	•064310	•119388
•3162	•444320	•249391	•121917	•092946	•057678	•109113
•3311	•445263	•249051	•119456	•090938	•052265	•099744
•3467	•446292	•250140	•117104	•089681	•048310	•091645
•3631	•447494	•252470	•115158	•088768	•045769	•084960
•3802	•448531	•255491	•113695	•088001	•044417	•079640
•3981	•448387	•258371	•112466	•087157	•043940	•075455
•4169	•445484	•260217	•111101	•086088	•043982	•072014
•4365	•438210	•260414	•109224	•084721	•041180	•068854
•4571	•425635	•258990	•106724	•083040	•044222	•065594
•4786	•408082	•256722	•103843	•081064	•043925	•062105
•5012	•387336	•254792	•101149	•078838	•043264	•058539
•5248	•366364	•254197	•099361	•076440	•042313	•051559
•5495	•348392	•255398	•099044	•074020	•041168	•052115
•5754	•335259	•258302	•100293	•071762	•039935	•045373
•6026	•325524	•262226	•102371	•069779	•038754	•046681

PULSE HEIGHT	2.98 MEV	3.96 MEV	5.97 MEV	8.12 MEV	11.0 MEV	14.4 MEV
•6310	•313440	•265759	•104441	•068052	•037753	•044738
•6607	•290157	•266994	•105089	•069445	•036946	•043154
•6918	•248078	•264266	•106579	•064748	•036226	•042223
•7244	•187183	•256943	•106851	•062779	•035509	•041719
•7586	•119220	•245772	•106430	•060642	•034858	•041020
•7943	•061445	•232711	•104929	•058789	•034427	•039262
•8318	•024686	•220072	•102419	•057527	•034283	•035885
•8710	•007484	•209046	•099587	•056520	•034331	•031274
•9120	•001665	•198282	•097095	•055200	•034431	•026715
•9550	•000265	•183126	•095327	•053484	•034564	•023401
1.0000	•000030	•156736	•094596	•051957	•034765	•021518
1.0471	•000002	•115958	•095071	•051166	•034928	•020472
1.0965	•000000	•068686	•096513	•051116	•034860	•019729
1.1482	•000000	•030322	•098378	•051388	•034522	•019128
1.2023	•000000	•009375	•100252	•051614	•034036	•018627
1.2589	•000000	•001925	•102444	•051610	•033502	•018176
1.3183	•000000	•000250	•105725	•051178	•033020	•017779
1.3804	•000000	•000020	•109716	•050594	•032685	•017521
1.4454	•000000	•000001	•112092	•050837	•032278	•017444
1.5136	•000000	•000000	•109977	•052007	•031528	•017392
1.5849	•000000	•000000	•102685	•052913	•030685	•017299
1.6596	•000000	•000000	•092926	•052888	•030058	•017396
1.7378	•000000	•000000	•085038	•052362	•029625	•017732
1.8197	•000000	•000000	•080446	•051944	•029055	•018036
1.9055	•000000	•000000	•073245	•051980	•028134	•017908
1.9953	•000000	•000000	•054300	•052292	•027366	•017134
2.0893	•000000	•000000	•027399	•052148	•026921	•016140
2.1878	•000000	•000000	•008237	•051440	•026488	•015641
2.2909	•000000	•000000	•001349	•050679	•025993	•015666
2.3988	•000000	•000000	•000112	•050040	•026049	•015653

PULSE HEIGHT	2.98 MEV	3.96 MEV	5.97 MEV	8.12 MEV	11.0 MEV	14.4 MEV
2.5119	.000000	.000000	.000004	.048986	.026546	.015394
2.6303	.000000	.000000	.000000	.047610	.026307	.015327
2.7542	.000000	.000000	.000000	.045640	.025799	.015584
2.8840	.000000	.000000	.000000	.039193	.026047	.015689
3.0200	.000000	.000000	.000000	.024551	.026973	.015165
3.3113	.000000	.000000	.000000	.001238	.027149	.014237
3.4674	.000000	.000000	.000000	.000063	.026439	.014107
3.6308	.000000	.000000	.000000	.000001	.025951	.014303
3.8019	.000000	.000000	.000000	.000000	.025835	.014561
3.9811	.000000	.000000	.000000	.000000	.025933	.014992
4.1687	.000000	.000000	.000000	.000000	.024219	.015249
4.3652	.000000	.000000	.000000	.000000	.021104	.014926
4.5709	.000000	.000000	.000000	.000000	.014496	.014699
4.7863	.000000	.000000	.000000	.000000	.004910	.015365
5.0119	.000000	.000000	.000000	.000000	.000508	.014969
5.2481	.000000	.000000	.000000	.000000	.000011	.014398
5.4954	.000000	.000000	.000000	.000000	.000000	.014036
5.7544	.000000	.000000	.000000	.000000	.000000	.013178
6.0256	.000000	.000000	.000000	.000000	.000000	.012389
6.3096	.000000	.000000	.000000	.000000	.000000	.011938
6.5069	.000000	.000000	.000000	.000000	.0000 0	.007941
6.9183	.000000	.000000	.000000	.000000	.000000	.001960
7.2444	.000000	.000000	.000000	.000000	.000000	.000102
7.5858	.000000	.000000	.000000	.000000	.000000	.000001
7.9433	.000000	.000000	.000000	.000000	.000000	.000000
8.3176	.000000	.000000	.000000	.000000	.000000	.000000
8.7096	.000000	.000000	.000000	.000000	.000000	.000000
9.1201	.000000	.000000	.000000	.000000	.000000	.000000
9.5499	.000000	.000000	.000000	.000000	.0000 0	.000000

APPENDIX B

Description and Explanation of the IBM-1410
Computer Program Used for Calculation of the
Response Functions

This computer code was written to convert the response functions as given in Appendix A from "Cobalt" pulse height units to channel pulse height units. A sub-program, INTERP, available from the KSU Computing Center, was used to interpolate between the given pulse height units for the desired response. The input and output parameters required for the execution of this program are given in Table B-I.

Table B-I

Input and Output Parameters Required for Execution of CONVERT

TIME	Normalization factor in first column of each response output
COBALT	Channel where compton edge from Cobalt-60 falls
IMAXTP	Number of pulse height unit values in data
NPTSTP	Number of points that INTERP will iterate on to fit a polynomial
XABCIS	Pulse height unit values as given in Appendix A
FORDIN	Probability of event per light unit as given in Appendix A
TVX	Calculated pulse height unit values in channel units
TVF	Calculated probability of event per channel

Execution time for this code varied from approximately 30 minutes

for 1 Cobalt = channel 20 to approximately 55 minutes for 1 cobalt = channel 200. Output from this code was in printed and punched form, 5E14.8 format. The punched output was used directly in the unfolding code.

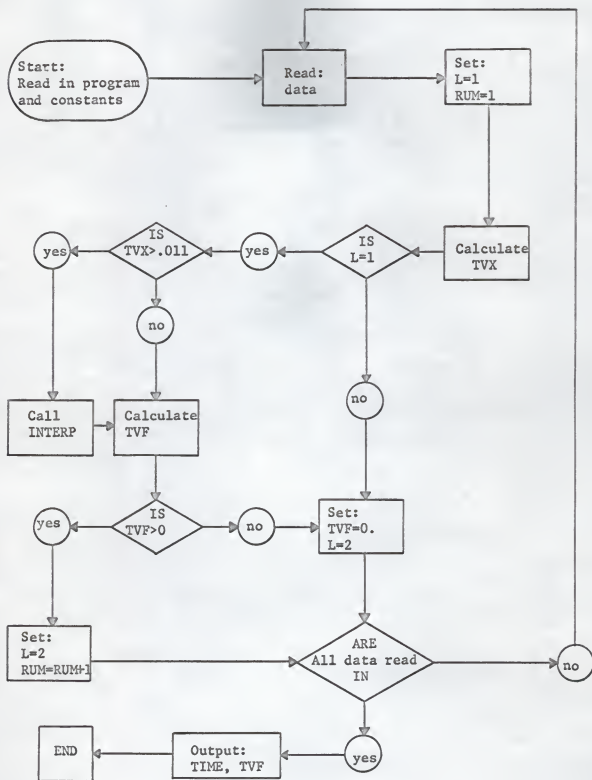


Figure 25. Logic diagram for program used to calculate the response functions

```

C      THIS PROGRAM CALCULATES THE RESPONSE MATRIX FOR 1 COBALT IN ANY
C      CHANNEL
C
C      DIMENSION XABCIS(200),FORDIN(200),SUM(200),TVX(200),TVF(200)
1  FORMAT(3I5)
2  FORMAT(1H ,5E14.8)
4  FORMAT(5E14.8)
5  FORMAT(F5.1)
6  FORMAT(10F8.4)
7  FORMAT(5E14.8)
C
C      MAIN PROGRAM TO CALL INTERP SUBROUTINE
C
C      TVX = PHU VALUES
C      TVF = PROBABILITY PER LIGHT UNIT
C      XABCIS = PHU FED IN AS DATA
C      FORDIN = PROBABILITY VALUES FED IN AS DATA
C      NPTSTP = NUMBER OF ITERATION POINTS ( 6 IN THIS CASE )
C      IMAXTP = NUMBER OF PHU VALUES IN DATA
C      TIME = NORMALIZATION FACTOR DESIRED IN FIRST COLUMN OF EACH ENERGY
C      COBALT = CHANNEL WHERE COMPTON EDGE FROM COBALT FALLS
C
8  READ(1,5)TIME
   READ(1,5)COBALT
   READ(1,1)IMAXTP,NPTSTP
   READ(1,6)(XABCIS(I),I=1,IMAXTP)
50  READ(1,4)(FORDIN(I),I=1,IMAXTP)
   L=1
   RUM=1.
   DO 300 I=1,200
     SUM(I)=RUM
     TVX(I)=SUM(I)/COBALT
     GO TO(10,275),L
10  IF(TVX(I).GT.0.011)GO TO 200
     J=I+1
     TVF(I)=(((FORDIN(J)-FORDIN(I)))/(XABCIS(J)-XABCIS(I)))*(TVX(I)-
C      (XABCIS(I)))+FORDIN(I)
     GO TO 250
200 CALL INTERP(IMAXTP,XABCIS,FORDIN,NPTSTP,TVX,TVF,I)
250 TVF(I)=TVF(I)/COBALT
     IF(TVF(I).GT.0.)GO TO 300
275 TVF(I)=0.
     L=2
300 RUM=RUM+1.
     WRITE(3,2)TIME,(TVF(I),I=1,200)
     WRITE(2,7)TIME,(TVF(I),I=1,200)
     GO TO 50
   END

```

```

SUBROUTINE INTERP(IMAXTP,XABCIS,FORDIN,NPTSTP,TVX,TVF,I)
DIMENSION XN(150),FN(150),FORDIN(200),XABCIS(200),TVX(200),TVF(2
C)
800 IF(IMAXTP-1)810,820,830
810 TVF(I)=0.
    GO TO 1000
820 TVF(I)=FORDIN(1)
    GO TO 1000
C   THESE ORDERS TAKE CARE OF ECCENTRICALLY SHORT LISTS
830 IF(NPTSTP-IMAXTP)850,840,840
840 NPTSTP=IMAXTP-1
C   ORDER OF INTERPOLATION IS DECREASED IF LIST IS TOO SHORT
850 XCTP=1.E90
    DO 890 INTP=1,IMAXTP
        ATP=TVX(I)-XABCIS(INTP)
        IF(ATP)860,870,870
860 ATP=-ATP
870 IF(ATP-XCTP)880,890,890
880 ITP=INTP
        XCTP=ATP
890 CONTINUE
C   THIS LOOP SELECTS THE VALUE OF XABCIS CLOSEST TO TVX
    IF (IMAXTP-ITP-1)892,892,889
889 IF(ITP-1)892,892,891
891 IF(ABS(TVX(I)-XABCIS(ITP+1))-ABS(TVX(I)-XABCIS(ITP-1)))892,892
    1,893
892 INNTP=1
    GO TO 894
893 INNTP = -1
894 NPTSTP=NPTSTP+1
C   THESE ORDERS DETERMINE ON WHICH SIDE OF TVX IS THE NEXT XABCIS
    DO 970 INTP=1,NPTSTP
        XN(INTP)=XABCIS(ITP)
        FN(INTP)=FORDIN(ITP)
        IF(INNTP)900,900,910
900 IQTP=ITP-INTP
    GO TO 940
910 IQTP=ITP+INTP
920 IF(IMAXTP-IQTP)930,940,940
930 ITP=ITP-1
    GO TO 970
940 IF(IQTP)950,950,960
950 ITP=ITP+1
    GO TO 970
960 ITP=IQTP
    INNTP=-INNTP
970 CONTINUE
C   THIS LOOP ORDERS THE INTERPOLATION POINTS
C   FOR INCREASING DISTANCES FROM TVX
    NPTSTP=NPTSTP-1

```

```
TVF(I)=0.
FACT=1.
DC 990 JNTP=1,NPTSTP
TVF(I)=TVF(I)+FACT*FN(I)
DC 980 INTP=JNTP,NPTSTP
IQTP=INTP-JNTP+1
980 FN(IQTP)=(FN(IQTP+1)-FN(IQTP))/(XN(INTP+1)-XN(IQTP))
990 FACT=FACT*(TVX(I)-XN(JNTP))
C THIS IS THE MAIN LOOP FOR CALCULATING THE DIVIDED DIFFERENCES
1000 RETURN
END
```

APPENDIX C

Explanation of the Input Routines for the IBM-1410
Unfolding Code Being Developed in the KSU Department
of Nuclear Engineering

The unfolding code used for this work was written by Eckhoff and Hill (8), KSU Nuclear Engineering staff members, to unfold complex spectra in the least squares sense, and to solve for errors in the unfolded spectra which result from statistical errors in the complex spectra. Presently under further development, the code contains several options especially designed for gamma-ray spectrum unfolding; these options were not used for the neutron spectra unfolding here and will not be explained.

Execution time for this program varied from approximately 20 minutes to 45 minutes, depending on the number of monoenergetic spectra and the nature of a particular solution. Output was in both printed and punched form. The input routines used for this work are given in Table C-I.

Table C-I

Input Routines for KSU Department of Nuclear Engineering Unfolding Code

Card or Deck	Columns	Information
Card 1:	1-3	Number of channels
	4-6	Number of monoenergetic spectra
	7-9	1 read in weighting factors
		2 weighting factors of unity
		3 weighting factors of $1/\beta$
	10-12	1 calculated spectra are printed
		0 calculated spectra are not printed
	13-15	Lower channel limit of least squares fit
	16-18	Upper channel limit of least squares fit
	19-21	1 one iteration on beta vector
	22-24	1 spectra read in on 8F10.0 Format
		0 spectra read in on 5E14.8 Format
	25-27	1 calculate standard deviation for spectra
		0 standard deviation not calculated
Card 2:	1-80	Any identification desired
Complex spectra deck:		5E14.8 or 8F10.0 Format--1st number is counting time
Weighting factors:		Usually not read in (see Card 1, Cols 7-9)
Identification of complex spectra:		Consecutive numbers to identify complex spectrum (15I3 Format)
Monoenergetic spectra:		5E14.8 or 8F10.0 Format--1st number of each energy = 1.0

APPENDIX D

Letter Received from Oak Ridge National
Laboratory Regarding KSU Data Analysis

The following letter was received from ORNL in reply to a KSU letter which submitted a Po-Be pulse height spectrum.

Much progress has been made since then in lowering the Forte circuit cut-off point; to date this cut-off point is approximately 0.15 cobalts for the KSU system.

OAK RIDGE NATIONAL LABORATORY

OPERATED BY

UNION CARBIDE CORPORATION

NUCLEAR DIVISION

POST OFFICE BOX X
OAK RIDGE, TENNESSEE 37831

May 5, 1966

Mr. Kenneth E. Habiger
Department of Nuclear Engineering
Kansas State University
Manhattan, Kansas

Dear Mr. Habiger:

I am sorry that we have taken so long to reply to your letter which submitted a Po-Be pulse-height spectrum and a stack of punched cards, but we have been totally occupied with a rather vital series of experiments relating to the proper analysis of our own NE-213 data.

We began looking at your spectrum by plotting the data and comparing it with our most recent Po-Be calibration run. We immediately observe that although we are in more or less rough agreement over the low-gain "bite," our curves do not match at all in the high-gain segment. The trouble seems to lie in the operation of your Forte circuit, which appears to be cutting off counts at 0.5 cobalts or even higher. The result of this is that very little useful information is obtained from your high-gain run. For comparison, the enclosed plot shows that we do not experience Forte turnover until around 0.025 cobalts. (Our data is shown in colored pencil, yours in black.)

Since our FERDO analysis of pulse-height curves similar to that shown (as our data) has resulted in unfolded Po-Be spectra which agree in most details with the more or less accepted spectrum of Whitmore and Baker [Phys. Rev. 78, 799 (1950)] we feel that some sort of similar pulse-height results will be necessary before any attempt is made to use the FERDO code. Accordingly, I will await further word from you before making any attempt to process the data.

Although we can offer no immediate suggestions concerning the problem, the disparity in the appearances of your high-gain and low-gain ^{60}Co data

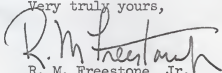
Mr. Kenneth E. Habiger

-2-

May 5, 1966

at the low-energy end is somewhat upsetting. We do not expect to see this, but rather curves which are basically the same. Further study is indicated here.

Very truly yours,


R. M. Freestone, Jr.
Neutron Physics Division

Encl.

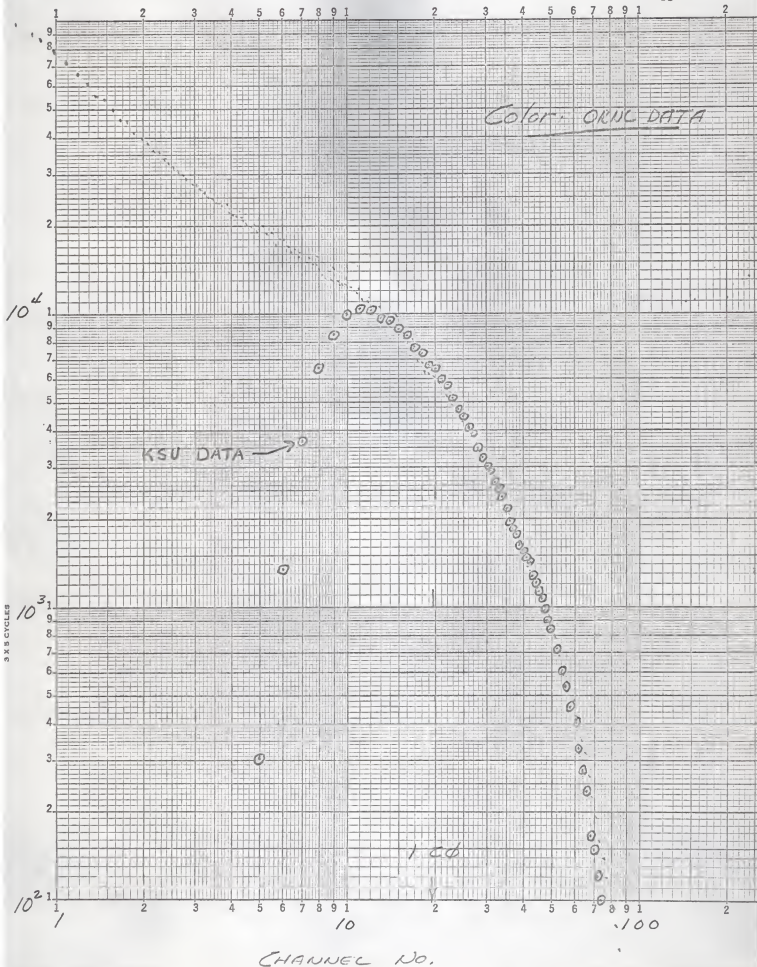
RMF:vg

cc: C. E. Clifford
W. R. Klmel (KSU)
V. V. Verbinski

HABIGER-K-STATE

Po-Be Low Gain

85



APPENDIX E

Modifications in the B. J. Electronics A8 Amplifier

THE MEASUREMENT OF THE FAST NEUTRON FLUX AT THE FAST
BEAM PORT OF THE KSU TRIGA MARK II REACTOR

by

Kenneth Edward Habiger

B. S., Kansas State University, 1964

AN ABSTRACT OF
A MASTER'S THESIS

Submitted in partial fulfillment of the
requirements for the degree

MASTER OF SCIENCE

Department of Nuclear Engineering

KANSAS STATE UNIVERSITY
Manhattan, Kansas

1966

ABSTRACT

A study was made of the operating characteristics and parameters of an NE-213 fast neutron spectrometer system, capable of discriminating against gamma-rays; the system was then applied to the measurement of the fast neutron spectra of Po-Be neutrons and reactor neutrons at the fast beam port of the KSU TRIGA Mark II reactor.

The gamma-ray discriminating circuit ("Forte circuit") was adjusted in conjunction with the baseline setting on a linear amplifier to maintain a 1000:1 gamma-ray rejection ratio and detect neutrons of the lowest possible energy. Photomultiplier tube voltages of 2300 volts or less were low enough to prevent phototube saturation from 14 Mev neutrons.

Po-Be and reactor neutron complex spectra were recorded with a multi-channel analyzer at two linear amplifier gains. The low gain complex spectra were characterized by a "peaking" effect in the higher channels due to high energy gamma leakage when operating the system under certain conditions. The peaking effect was smoothed using spectra recorded when peaking did not occur.

The low gain complex spectra were successfully unfolded in the 1.5 to 14 Mev neutron energy range using a code being developed in the KSU Department of Nuclear Engineering. High gain unfolding attempts were unsuccessful due to the probable difference in resolution between the KSU NE-213 system and the resolution characteristic of the unfolding code response function data.

Resolution for the system can be improved by replacing the white

reflector paint on the scintillator bottle with aluminum foil. In addition, response of the system to monoenergetic neutrons should be measured to determine the reliability of the unfolding code response function data.